Tuomas Paloposki & Leif Liedquist

Steel emissivity
at high temperatures

Steel emissivity at high temperatures

Tuomas Paloposki

VTT Building and Transport

Leif Liedquist

SP Measurement Technology

Abstract

A new test method was developed at VTT for the determination of the emissivities of different types of steel and other metallic materials as a function of the temperature of the material. The method is simple and inexpensive, but its use is limited to materials which possess a high thermal conductivity and are physically and chemically inert in the temperature range of interest (no melting or other phase transitions, no charring, burning or other chemical reactions). Furthermore, reliable results are only obtained above a minimum temperature, the value of which varies depending on experimental conditions but seems to be in the range from 150 ℃ to 200 ℃.

Three different steel types were used in testing the new method: two stainless steels and one carbon steel. The emissivities of the two stainless steels were determined for the temperature range from approximately 200 ℃ to approximately 600 ℃. The emissivity of the carbon steel was determined for the temperature range from approximately 150 ℃ to approximately 550 ℃.

Uncertainty of the emissivity values obtained with the new method was estimated to be approximately ±20 %. Repeatability of the results was well within the ±20 % limit.

The results were compared with those obtained using a method developed earlier by SP. The SP method gives emissivity at a fixed temperature; earlier the fixed temperature was 100 ℃, but the method was now upgraded so that 200 ℃ also became possible. Thus, emissivity values at 200 ℃ could be used to compare the two methods.

For the two stainless steels, there was good agreement between results obtained using the new method and results obtained using the existing method. For the carbon steel, the differences were much larger than would have been expected. The reasons for the differences have not been found yet and should be further investigated.

Sammanfattning

En ny provmetod har utvecklats hos VTT för mätning av emissivitet hos olika sorter av stål och andra metaller. Emissiviteten mäts som funktion av materialets temperatur. Metoden är enkel och billig, men kan endast tillämpas för materialer som har hög värmekonduktivitet och som är fysikaliskt och kemiskt passiva, dvs som inte genomgår smältning eller andra fastransformationer och som inte förkolnas, bränns eller deltar i andra kemiska reaktioner. Härtill kan pålitliga resultat endast nås ovanför en minimumtemperatur, som varierar enligt provförhållanden men verkar vara ungefär 150…200 ℃.

Tre olika sorter av stål användes i testerna: två typer av rostfritt stål och ett byggnadsstål. För de två typerna av rostfritt stål, mättes emissiviteter inom temperaturområdet 200…600 ℃ och för byggnadsstålet inom temperaturområdet 150…550 ℃.

Osäkerheten i emissivitetsvärden som mättes med den nya metoden uppskattades vara ungefär ±20 %. Reproducerbarheten var tydligt inom de här gränserna.

Resultaten jämfördes med de resultat som nåtts med en existerande metod tidigare utvecklad hos SP. Den existerande metoden producerar emissivitetsvärden vid en bestämd temperatur; tidigare var den bestämda temperaturen 100 ℃, men nu utvecklades metoden så att emissiviteten kan också mätas vid 200 ℃. Så blev det möjligt att jämföra resultat som nåtts med de två metoderna.

För de två typerna av rostfritt stål, passade resultaten som nåtts med den nya metoden bra ihop med resultaten som nåtts med den existerande metoden. För byggnadsstålet var skillnaderna större än väntat. Orsakerna till skillnaderna är inte ännu kända och borde studeras.

Preface

Contents

List of symbols

A surface area; cross-sectional area

c specific heat; constant in Equations (35) and (36)

D diameter

F configuration factor

g gravitational constant

Gr   Grashof number

h heat transfer coefficient

L length

m mass; parameter defined in Equation (29); exponent in Equation (33)

n exponent in Equation (33)

Nu   Nusselt number

P perimeter

Pr   Prandtl number

$\dot{Q}$ heat flow

$\dot{q}$ heat flux

Ra   Rayleigh number

S thickness

T temperature

t time

u uncertainty

V volume; voltage

W width

x variable; spatial coordinate

y variable

γ ratio of original surface area to total surface area

ε emissivity

λ thermal conductivity; wavelength

μ dynamic viscosity

ν kinematic viscosity

ρ	reflectance
σ	Stefan-Boltzmann constant

Subscripts

A	fluid surrounding the test specimen
a	ambient
b	blackbody
Cond	conductive
Conv	convective
c	chopper blade
f	furnace
Int	internal
M	material of the test specimen
m	material of the test specimen
N	normal
o	original
p	constant pressure
Rad	radiative
s	settling period
t	tube
tot	total
W	wire
0	initial
1	test specimen
2	cavity (or furnace) walls

1. Introduction

1.1 Background

Buildings need to be aesthetically pleasing yet efficient, and they should be constructed at reasonable costs. New and innovative structures utilizing various types of steels and other metallic materials are continually being developed to reach these objectives.

In the case of a fire, the safety of the people occupying the building depends on the ability of the structure to perform its duties for a sufficiently long time, e.g. to maintain load bearing capability, insulation capability and integrity. The performance of a steel structure during a fire very much depends on the rate at which the structure heats up due to the heat transfer from the fire to the structure. In many cases, thermal radiation is a significant mode of heat transfer; thus, the radiative properties of the steel are directly related to the fire safety of the structure.

However, the radiative properties of construction materials have only attracted rather limited attention. For example, the building codes in Nordic countries traditionally include simplified calculation procedures for the analysis of load-bearing steel structures. The radiative properties of the steel do not appear explicitly in the equations presented in the building codes and it is not possible to apply different values depending on the steel type or surface finish. This simplification has been quite useful and understandable in the past, but we should now set our aims higher. It is to be expected that as our computational resources and our understanding of fires and their development are increasing, we will eventually be able to develop more advanced analysis methods which fully utilize new information on radiative properties of actual materials in the temperature range from room temperature up to fire temperatures. The advantages of such methods are by no means limited to the development of load-bearing structures but also open up new possibilities in the development of other building products, e.g., separating doors etc.

1.2 About terminology

The radiative properties of an opaque surface include absorptivity, emissivity and reflectivity, all of which may be functions of the temperature of the surface and of the direction and wavelength of the radiation being received or emitted; thus, an attempt to completely specify the radiative properties of a steel surface will result in quite an overwhelming amount of information. However, the situation can be greatly simplified if we are just interested in computing the radiative heat transfer between a steel structure and its surroundings during a fire. For this purpose, the important properties are the

hemispherical total absorptivity and hemispherical total emissivity of the steel (here hemispherical means radiation integrated over all directions and total means radiation integrated over all wavelengths). Furthermore, if certain conditions are met, then the hemispherical total absorptivity is equal to the hemispherical total emissivity; this is a special case of the Kirchhoff's law. The conditions have been listed, e.g., in Table 3-2 of Siegel and Howell (1972).

From now on, it will be assumed that for all materials analyzed in this study, the hemispherical total absorptivity is equal to the hemispherical total emissivity, and this quantity will be called emissivity. The attributes directional and spectral will be employed whenever dependence on direction or wavelength needs to be considered.

1.3 Objective

The objective of this study was to develop a simple and inexpensive method for the determination of the emissivities of various types of steel and other metallic materials as a function of their temperature, from room temperature up to fire temperatures.

1.4 Organization

The development of the new method was carried out by VTT Building and Transport in Finland. The results obtained using the new method were compared with those obtained using an existing method developed earlier by SP in Sweden.

It is anticipated that the new method itself and the results produced by the new method will be utilized by construction products industry, building designers and building authorities.

2. Comparison of the methods

2.1 Existing method (SP method)

The SP method was developed in 1979 for one specific purpose: characterisation of solar collector absorbers in emissivity. The basic idea with the SP method was to have a tool to measure emissivity of a larger number of different materials in a cost effective way, i.e. a method with fast measurements. The development of the SP method has been described by Sidsten (1979) and Liedquist (1987).

2.1.1 Description of the existing method

The principle of the SP method is the following. The normal component of the emissivity is measured. Spectrally total emissivity is achieved by using a spectrally flat and broadband infrared detector, The material, which must be metallic and flat, is heated to about 100 °C by pressing it toward a heated aluminum body. The detecting system measures the radiance alternatively from the sample and from a blackbody. The latter is also set at about 100 °C. The emissivity is calculated in principle by simply taking the ratio of the two detector outputs. However, a few corrections must be made. The equipment and the procedure are described in detail in Chapter 7.

A modification of the existing method was also carried out as part of this study. The modification allows the emissivity to be determined at any temperature within the range 100…200 °C. The modification is also described in Chapter 7.

2.1.2 Advantages of the existing method

The method has relatively high accuracy. For high emissivities, the accuracy is limited by the uncertainty of the measurement of the surface temperature and for low emissivities by the uncertainty of the radiance contribution from the surroundings. The total uncertainty in the measurement of total normal emissivity is 0.05 for high emissivities and 0.02 for low emissivities.

The method has turned out to be quick and reliable. It has been used by SP since 1980, mainly for measurement of directional emissivity of solar collector absorbers, and is still in use for this purpose.

Materials with flat but non-homogenous structure of the surface can be measured, since the detector measures the radiance being emitted by a spot with a diameter of less than 7 mm.

2.1.3 Disadvantages of the existing method

The method uses equipment that are normally only available in laboratories specializing in optical measurements, such as a Golay detector having KRS5 window, a lock-in-amplifier and special temperature measurement equipment.

Emissivity is obtained at a fixed temperature. In the original setup only one temperature, 100 °C, is permitted. However, with the modifications carried out in this study, any temperature within the range 100 °C–200 °C could be set and used. Perhaps 300 °C would be possible but because of the manual handling of the samples it could be very inconvenient for the operator to handle the materials at that high temperature.

In spite of the additional features of the method the temperature range is very limited to what is needed. A radiometric method for higher temperatures would require a completely different method which is not available at SP for the time being.

2.2 New method (VTT method)

2.2.1 Description of the new method

The method is based on the following procedure. The test specimen is a small body made of the material whose emissivity is to be determined. The test specimen is initially at room temperature and is then suddenly placed inside a hot furnace. As the test specimen heats up due to heat transfer from the hot furnace, its temperature is recorded as a function of time. The emissivity of the material can be deduced from the temperature – time data provided that certain conditions are met. Chapters 3 and 4 are devoted to describing how all this shall be done, what the limitations are and what practical matters must be taken into consideration in such experiments.

2.2.2 Advantages of the new method

The new method is quite simple and does not require special equipment. Basically, all that is needed is a laboratory furnace, a data logger for temperature measurements, and a

mechanical workshop for preparing the test specimens. Details of the equipment and of the design and preparation of the test specimens will be discussed in Chapters 4 and 6.

With the new method, each experiment produces a set of data which can be used to obtain the emissivity of the material as a function of its temperature. Thus, a large amount of information can be collected quickly.

The surface of the test specimen does not need to be flat. However, the mathematical analysis presented in this study is limited to test specimens having convex surfaces.

2.2.3 Disadvantages of the new method

The accuracy of the new method is not expected to be particularly good. Reasons for this will become clear in Chapters 3 and 4.

The emissivity of the test material should be the same at all surfaces. This could become a problem in some cases, for instance, when studying materials which have a specific treatment applied to just one of the surfaces.

The test material should possess a high thermal conductivity. In practice, metallic materials are acceptable. This point will be discussed in Section 4.5.

The test material should be physically and chemically inert in the temperature range of interest (no melting or other phase transitions, no charring, burning or other chemical reactions). It must be added, of course, that the determination of the emissivities of materials undergoing physical or chemical transitions is quite difficult by any method.

3. Theoretical analysis of the new method

This chapter presents a theoretical analysis of the heat transfer processes for an idealized case described in Section 3.1. The practical implementation of the experiments will be discussed in Chapter 4; the experimental setup and procedure developed at VTT will be described in Chapter 6.

3.1 Test setup

Consider the situation shown in Figure 1. A small body is initially at room temperature, and at time $t = 0$ the body is inserted into a hot cavity. Let T_1 be the temperature of the body and T_2 be the temperature of the cavity[1]. Both T_1 and T_2 are recorded as functions of time t. Assume for time being that both the body and the cavity are spherical and concentric.

The heat transfer processes between the relatively cool body and its hot environment will be analyzed in Section 3.2; after that, the energy balance for the body will be formulated in Section 3.3. It will turn out that the emissivity of the material, of which the body is made of, can be computed in a relatively straightforward manner from the measured values of $T_1(t)$ and $T_2(t)$, provided that certain conditions are met. The conditions will be discussed in this and the following chapter.
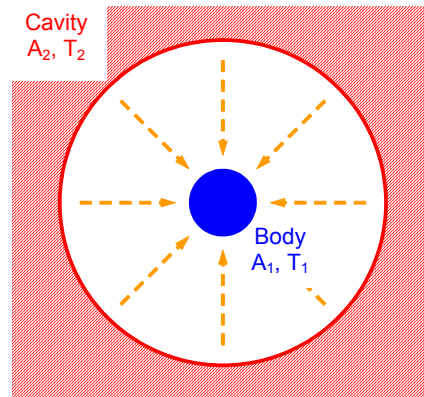
Figure 1. A schematic view of the experimental setup of the new method for the determination of emissivity. A small body is inserted into a hot cavity, and the temperatures of the body and the cavity are recorded as functions of time.

---

[1] Throughout this study, the subscripts 1 and 2 are used to denote the body and the cavity, respectively.

3.2 Heat transfer processes

3.2.1 Radiation

Consider the radiative heat transfer between two concentric spheres as were shown in Figure 1. Assume that the surface of the inner sphere is at a uniform temperature T_1 and that the surface of the outer sphere is at a uniform temperature T_2. Let A_1 and ε_1 be the surface area and emissivity of the inner sphere, respectively, and A_2 and ε_2 be the surface area and emissivity of the outer sphere, respectively. Also assume that the surfaces of the spheres are diffuse-gray.

This problem has been presented as Example 8-3 in the textbook of Siegel and Howell (1972) to illustrate the use of the net radiation method for the solution of radiative heat transfer problems. The net radiative heat flow supplied to the smaller sphere is shown to be

$$\dot{Q}_{rad} \quad = \quad \frac{A_1 \sigma (T_2^4 - T_1^4)}{\dfrac{1}{\varepsilon_1(T_1)} + \dfrac{A_1}{A_2}\left[\dfrac{1}{\varepsilon_2(T_2)} - 1\right]} \tag{1}$$

where σ is the Stefan-Boltzmann constant ($5.67 \cdot 10^{-8}$ W/(m^{2}K^4)). The notation has been chosen to emphasize the fact that the emissivities of both spheres may be functions of temperature. Here the sign has been chosen to be positive for the case where the inner sphere is a net receiver of energy ($T_2 > T_1$) and negative for the case where the inner sphere is a net supplier of energy ($T_2 < T_1$).

Equation (1) is not very practical, since using it requires that we know the value of the emissivity of the furnace liner $\varepsilon_2(T_2)$. Usually we do not. However, if the size of the inner sphere is small when compared to the size of the outer sphere and if the emissivity of the outer sphere is not very small, Equation (1) simplifies to

$$\dot{Q}_{rad} \quad = \quad \varepsilon_1(T_1) A_1 \sigma (T_2^4 - T_1^4) \tag{2}$$

which means that the net radiative heat flow is independent of the emissivity of the outer sphere. This result was also derived by Siegel and Howell.

3.2.2 Conduction

Consider the conduction of heat between two concentric spheres as were shown in Figure 1. Assume that the space between the spheres is filled with a fluid whose thermal conductivity is λ_A. Assume that the surface of the inner sphere is at a uniform temperature T_1 and the surface of the outer sphere is at a uniform temperature T_2. Let D_1 and D_2 be the diameters of the inner and outer spheres, respectively.

The solution for this case has been presented in, for instance, VDI-Wärmeatlas (1984). The heat flow supplied to the smaller sphere is

$$\dot{Q}_{\text{Cond}} \quad = \quad \frac{2\pi\,\lambda_A(T_2 - T_1)}{\dfrac{1}{D_1} - \dfrac{1}{D_2}} \quad = \quad \frac{2\pi\,\lambda_A D_1(T_2 - T_1)}{1 - \dfrac{D_1}{D_2}} \tag{3}$$

which simplifies to

$$\dot{Q}_{\text{Cond}} \quad = \quad 2\pi\,\lambda_A D_1(T_2 - T_1) \tag{4}$$

when $D_1 \ll D_2$. Again, the sign has been chosen to be positive for the case where the inner sphere is receiving energy.

3.2.3 Convection

Consider a spherical body immersed in a fluid of large extent. Far away from the body, the fluid is assumed to be at rest and at temperature T_2. The surface area and the temperature of the body are A_1 and T_1, respectively. The temperature difference between the fluid and the body will induce a flow about the body; this flow will enhance the heat transfer between the body and the fluid above that obtained by mere conduction of heat. The phenomenon is called natural convection.

The convective heat transfer between the fluid and the body is normally expressed as

$$\dot{Q}_{\text{Conv}} \quad = \quad h_{\text{Conv}} A_1(T_2 - T_1) \tag{5}$$

where h_{Conv} is the convective heat transfer coefficient between the fluid and the body. The sign has been chosen to be positive for the case where the body is receiving energy from the fluid.

As will be seen below, the expression for the convective heat transfer coefficient is formulated in such a manner that it also takes into account the heat conduction between the body and its surroundings. Thus, Equation (5) also includes the contribution by heat conduction expressed in Equation (3).

The value of the convective heat transfer coefficient is solved in the following manner. VDI-Wärmeatlas (1984) gives the following equation to describe the heat transfer by natural convection between a fluid and a spherical body immersed in the fluid:

$$\mathrm{Nu} = \left\{ 1.414 + \frac{0.387 \, \mathrm{Ra}^{1/6}}{\left[1 + \left(\frac{0.492}{\mathrm{Pr}} \right)^{9/16} \right]^{8/27}} \right\}^2 \tag{6}$$

where Nu is the Nusselt number, Ra is the Rayleigh number and Pr is the Prandtl number. They are defined as follows.

The Nusselt number is defined as

$$\mathrm{Nu} = \frac{h_{\mathrm{Conv}} L}{\lambda_{\mathrm{A}}} \tag{7}$$

where h_{Conv} is the convective heat transfer coefficient between the fluid and the body, L is the characteristic dimension of the body and λ_{A} is the thermal conductivity of the fluid. In the case of a spherical body, L is equal to the diameter of the body (in the case being considered here, $L = D_1$).

The Rayleigh number is defined as

$$\mathrm{Ra} = \mathrm{Gr} \cdot \mathrm{Pr} \tag{8}$$

where Gr is the Grashof number and Pr is the Prandtl number. If the fluid can be assumed to behave as an ideal gas, then the Grashof number can be expressed as

$$\mathrm{Gr} = \frac{g L^3}{v_{\mathrm{A}}^2} \frac{T_2 - T_1}{T_2} \tag{9}$$

where g is the gravitational constant (9.81 m/s^2), L is the characteristic dimension of the body, v_{A} is the kinematic viscosity of the fluid and T_2 and T_1 are the temperatures of the fluid and the body, respectively. In the case of a spherical body, L is equal to the diameter of the body (in the case being considered here, $L = D_1$).

The Prandtl number is defined as

$$\text{Pr} \;=\; \frac{\mu_A c_{pA}}{\lambda_A} \tag{10}$$

where μ_A, c_{pA} and λ_A are the dynamic viscosity, the specific heat and the thermal conductivity of the fluid, respectively.

Thus, Equations (6)–(10) can be used to solve for the convective heat transfer coefficient h_{Conv}. All thermal properties of the fluid are to be taken at the average temperature between the fluid and the body $\overline{T} = (T_1 + T_2)/2$.

It is of interest to compare the relative magnitudes of convection heat transfer and conduction heat transfer in this case. Inserting Equation (7) into Equation (5) gives

$$\dot{Q}_{\text{Conv}} \;=\; h_{\text{Conv}} A_1 (T_2 - T_1) \;=\; \frac{\text{Nu}\,\lambda_A}{D_1} \pi D_1^2 (T_2 - T_1) \;=\; \text{Nu}\,\pi\,\lambda_A D_1 (T_2 - T_1) \tag{11}.$$

Since the fluid is assumed to be of large extent, Equation (4) can be used to describe conduction heat transfer. Thus, the ratio of convection heat transfer to conduction heat transfer is

$$\frac{\dot{Q}_{\text{Conv}}}{\dot{Q}_{\text{Cond}}} \;=\; \frac{\text{Nu}\;\pi\;\lambda_A\,D_1\,(T_2 - T_1)}{2\,\pi\lambda_A\,D_1\,(T_2 - T_1)} \;=\; \frac{\text{Nu}}{2} \tag{12}.$$

Now for $T_1 \to T_2$, the importance of the flow induced by the temperature difference decreases and the value of $\dot{Q}_{\text{Conv}}$ should therefore approach that of $\dot{Q}_{\text{Cond}}$. This is indeed found to be the case, since $\text{Gr} \to 0$ for $T_1 \to T_2$ and therefore $\text{Nu} \to 2$ which gives $\dot{Q}_{\text{Conv}} \approx \dot{Q}_{\text{Cond}}$. This observation is in accordance with the earlier statement that the equations of natural convection are normally formulated in such a manner that they also take into account the heat transfer by conduction. When the temperature difference between the fluid and the body becomes larger, then the values of Gr and Nu increase, which reflects the fact that the relative importance of convection increases.

3.3 Energy balance for the test specimen

In this section, the energy balance for a small spherical body inserted in a hot cavity filled with a fluid is presented using the expressions derived in Section 3.2.

Assume that although the temperature of the body increases with time, at any instant of time the body is at a uniform temperature T_1. Thus, the energy balance for the body may be written as

$$m_1 c_{p1} \frac{dT_1}{dt} = \sum_i \dot{Q}_i \tag{13}$$

with the initial condition

$$T_1 = T_0 \quad \text{at} \quad t = 0. \tag{14}$$

In Equations (13) and (14), m_1 is the mass of the body, c_{p1} is the specific heat of the material of the body, t is the time, and $\dot{Q}_i$ are the heat flows between the body and its environment.

The heat flows between the body and its environment are the radiative heat flow $\dot{Q}_{\text{Rad}}$ presented in Equation (2) and the convective heat flow $\dot{Q}_{\text{Conv}}$ presented in Equation (5). As was discussed in Section 3.2.3, the convective heat flow also includes $\dot{Q}_{\text{Cond}}$, the contribution by heat conduction.

Thus, substitution into Equation (13) gives

$$m_1 c_{p1} \frac{dT_1}{dt} = \dot{Q}_{\text{Rad}} + \dot{Q}_{\text{Conv}} = \varepsilon_1(T_1) A_1 \sigma (T_2^4 - T_1^4) + h_{\text{Conv}} A_1 (T_2 - T_1) \tag{15}$$

from which the emissivity $\varepsilon_1(T_1)$ can be solved as

$$\varepsilon_1(T_1) = \frac{m_1 c_{p1} \frac{dT_1}{dt} - h_{\text{Conv}} A_1 (T_2 - T_1)}{A_1 \sigma (T_2^4 - T_1^4)} \tag{16}$$

To summarize, the emissivity of a material can be determined from experimental data if m_1, A_1 and c_{p1} are known, $T_1(t)$ and $T_2(t)$ are measured and recorded during the experiment, and h_{Conv} is computed using the procedure presented in Section 3.2.3. Practical implementation of such experiments will be discussed in Chapter 4.

4. Practical considerations of the new method

4.1 Furnace type

The most practical choice for the test furnace is an electrically heated laboratory furnace. A spherical furnace chamber would be desirable from the point of view of achieving a uniform thermal radiation field inside the furnace (cf. Section 3.2.1), but normally furnaces are built with rectangular or cylindrical furnace chambers. The advantage of a rectangular furnace chamber is that having a furnace chamber with a flat floor makes it easier to design and to operate the specimen holder which is needed to support the test specimen inside the furnace.

4.2 Furnace size

The minimum size of the furnace is determined by the condition that the emissivity of the furnace liner must be eliminated from the equation describing the radiative heat transfer between the furnace walls and the test specimen; in other words, it must be possible to use Equation (2) instead of Equation (1). In mathematical terms, it must be required that

$$\frac{A_1}{A_2}\left[\frac{1}{\varepsilon_2(T_2)}-1\right] \;<<\; \frac{1}{\varepsilon_1(T_1)} \tag{17}$$

which can be rearranged to

$$\frac{A_2}{A_1} \;>>\; \varepsilon_1(T_1)\left[\frac{1}{\varepsilon_2(T_2)}-1\right] \tag{18}.$$

Here A_1 and ε_1 are the surface area and emissivity of the test specimen, respectively, and A_2 and ε_2 are the surface area and emissivity of the furnace walls, respectively. The emissivities of furnace liner materials are typically between 0.3 and 0.7 (Incropera & DeWitt 2002). The emissivities of steel and other metallic materials are expected not to be higher than approximately 0.85. Thus, the expression on the right side of Equation (18) is typically smaller than approximately 2, and Equation (17) will therefore be valid if A_2/A_1 is larger than approximately 100.

As will be discussed in Section 4.5, the surface area of the test specimen will typically be of the order of 20 cm^2. This means that the surface area of the furnace walls should

be at least of the order of 2000 cm², or, assuming a rectangular furnace chamber, the linear dimensions of the furnace chamber should be approximately 20 cm.

Another point to be observed is that the size of the furnace chamber should not be made any larger than what is necessary in view of considerations presented above. The reason is that one should try to minimize the effect of the thermal disturbance caused by the opening of the furnace door as the test specimen is inserted into the furnace. This point will be elaborated on in the next section.

4.3 Furnace temperature

The furnace must be capable of achieving a sufficiently high temperature so that the emissivity of the material to be investigated is obtained throughout the temperature range of interest. In the case of structural steel this usually means that the test specimen must be heated at least to a temperature of 500 ºC. The furnace temperature must be still higher; the experience gained at VTT indicates that the furnace temperature must be at least 100 ºC higher than the maximum temperature for which the emissivity is to be obtained. The reason is that as the temperature of the test specimen approaches the furnace temperature, the heating rate of the test specimen slows down and the relative uncertainty in evaluating the dT_1/dt term in Equation (16) becomes too large.

The furnace temperature should also be sufficiently high in order to ensure that radiative heat transfer is the dominant heat transfer mechanism; otherwise the numerator of Equation (16) will contain two quantities of almost equal magnitude and the results will be very sensitive to any errors made during the measurements. Thus, it has to be required that

$$\frac{\dot{Q}_{rad}}{\dot{Q}_{Conv}} \quad >> \quad 1 \tag{19}.$$

By applying Equations (2) and (5), we obtain

$$\frac{\dot{Q}_{rad}}{\dot{Q}_{Conv}} \quad = \quad \frac{\varepsilon_1 A_1 \sigma (T_2^4 - T_1^4)}{h_{Conv} A_1 (T_2 - T_1)} \quad = \quad \frac{\varepsilon_1 \sigma (T_2^4 - T_1^4)}{h_{Conv} (T_2 - T_1)} \tag{20}.$$

The parameters that can be controlled by the experimentalist are the furnace temperature T_2 and, to some extent, the convective heat transfer coefficient h_{Conv} (which is a function of the size and shape of the test specimen). In practice, however, the

possibilities for adjusting the value of h_{Conv} are quite limited. Thus, Equation (20) can be used to estimate what value for the furnace temperature T_2 is needed at different situations; an example of calculations with $\varepsilon_1 = 0.25$ and $h_{Conv} = 10$ W/m^{2}K is shown in Figure 2. For this particular case, the conclusion is that the temperature of the furnace should be at least 600 °C.

However, the furnace temperature should not be set any higher than what is necessary. There are two reasons for this:

- If the radiative heat flow to the test specimen is excessively high, then the temperature of the test specimen increases quite rapidly and a significant amount of data will be lost at the beginning of the test due to the disturbance caused the opening of the furnace door. This point will be discussed in more detail later in this section.

- If the radiative heat flow to the test specimen is excessively high, then the temperature gradients inside the test specimen will become too large for the energy balance equation to be meaningful. This point will be discussed in Section 4.5.
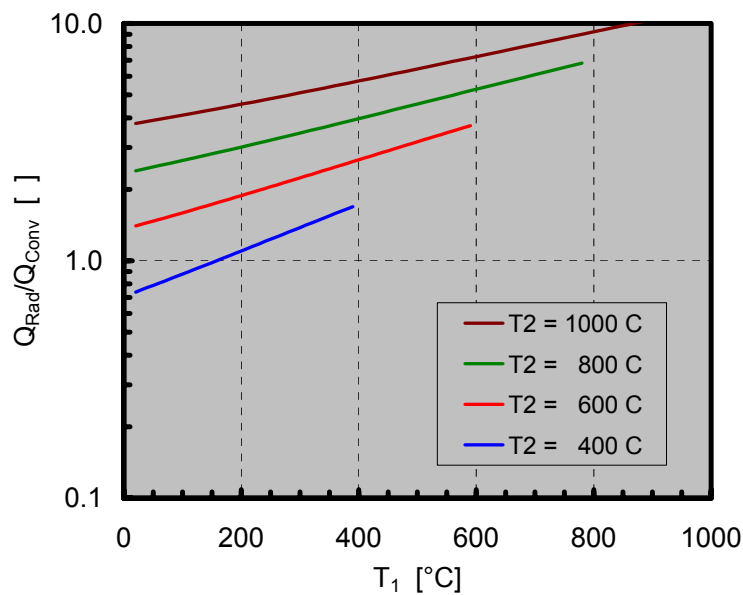
Figure 2. The ratio of the radiative heat flow to convective heat flow for different values of furnace temperature T_2. Here it has been assumed that the emissivity of the test specimen is 0.25 and that the convective heat transfer coefficient between the test specimen and air in the furnace is 10 W/m^{2}K.

One of the problems in choosing the appropriate furnace temperature is the thermal disturbance caused by the opening of the furnace door when the test specimen is

inserted into the furnace. The situation is illustrated in Figure 3. The test is started when the furnace has reached a steady state and both the walls of the furnace chamber and the air inside the furnace are at a uniform temperature. As the furnace door is opened, hot air flows out from the furnace and becomes replaced by cold ambient air. The walls of the furnace chamber will also cool down to some extent due to the inflow of cold air and due to radiation losses through the door opening. Thus, as the furnace door is closed again after the test specimen has been inserted into the furnace, the temperature of the air inside the furnace is lower than the temperature of the furnace walls. It can also be presumed that quite significant spatial variations exist in the wall temperatures; in particular, the temperature of the furnace door can be expected to be lower than the temperatures of the other walls.

After the furnace door has been closed, the temperature differences inside the furnace will even out within a certain period of time, the length of which depends on the size of the furnace chamber, on the thermal properties of the furnace walls, and on the heating and temperature control system of the furnace. This period is called the settling period. After the settling period, the temperatures of the air inside the furnace chamber and of the walls of the furnace chamber may still change with time (although such changes are expected to be rather slow), but spatial variations of furnace wall temperature and the temperature difference between the furnace walls and air are assumed to be negligible.
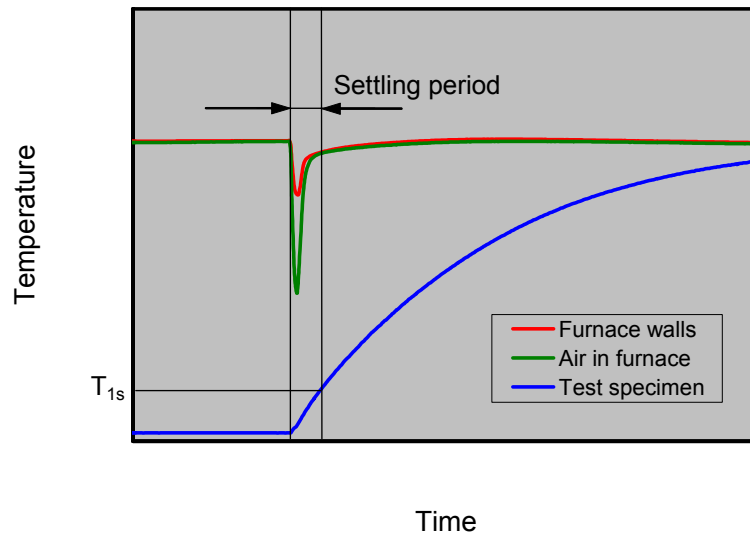
Figure 3. A schematic representation of the thermal disturbance caused by the insertion of the test specimen into the furnace.

The settling period is a problem since the experimental data are to be processed using Equation (16), which is only applicable if both the walls of the furnace chamber and the

air inside the furnace are at a uniform temperature T_2. This condition is not fulfilled during the settling period; thus, interpretation of the data which have been obtained during the settling period is practically impossible. Since the test specimen already heats up to some value temperature T_{1s} during the settling period, the consequence is that the emissivity of the material being studied is only obtained for temperatures $T_1 > T_{1s}$.

To keep the value of T_{1s} as small as possible, two methods can be used:

- The radiative heat flow from the furnace walls to the test specimen can be decreased by decreasing the furnace temperature. As was noted above, the temperature of the furnace should not be any higher than what is necessary from the point of view of having a sufficiently high radiative heat flow when compared to the convective heat flow.

- The surface-to-mass ratio of the test specimen can be decreased. In the case of a spherical test specimen, the diameter of the test specimen should be large; in a more general sense, the thickness of the test specimen should be large. It should be noted, however, that the test specimens should not be too thick. The problems associated with test specimen thickness will be further discussed in Section 4.5.

In principle, a third method is also available. As was noted in Section 4.2, the duration of the settling period also depends on the size of the furnace chamber. The dependence can be described in the following manner:

$$\Delta t_s \quad \propto \quad \frac{m_A}{\dot{Q}_A} \quad \propto \quad \frac{V_2}{A_2} \quad \propto \quad \frac{L_2^3}{L_2^2} \quad \propto \quad L_2 \tag{21}$$

where m_A is the mass of the air in the furnace chamber, $\dot{Q}_A$ is the heat flow from the walls of the furnace chamber to the air in the furnace chamber, and L_2, A_2 and V_2 are the linear dimension, surface area and volume of the furnace chamber, respectively. Thus, to minimize the duration of the settling period, the size of the furnace chamber should be small. However, the size of the furnace chamber is already determined by the requirement that the surface area of the furnace chamber should be large when compared with the furnace area of the test specimen (cf. Section 4.2). Thus, selection of the size of the furnace chamber cannot really be used as a means to shorten the duration of the settling period.

4.4 Supporting the test specimen in the furnace

During the experiments, the test specimens shall be placed inside the furnace chamber, and, for the theory described in Chapter 3 to be true, the location of the test specimens should be at or near the center of the furnace chamber. The easiest way to achieve this is to suspend the test specimen from the wires of the thermocouple which is being used for the measurement of the temperature of the test specimen. The thermocouple wires need to be supported by a specimen holder, which is placed inside the furnace together with the test specimen. Naturally, the disturbance caused by the specimen holder should be minimized.

The measurement of the temperatures of the test specimen and of the furnace chamber is discussed in Section 4.6. An analysis on the errors caused by heat conduction through the thermocouple wires is also presented there.

4.5 Test specimen shape and size

The main requirement for the test specimens is that they should preserve the essential characteristics of the surfaces of the materials to be studied. The test specimens should also be easy to manufacture.

The materials to be studied are various types of steel and other metallic materials, which are used as construction materials. Such materials are typically available as sheets, plates and profiles. Thus, the most practical shape for a test specimen is a slab or a flat block as shown in Figure 4. Spherical test specimens considered in the theoretical analysis presented in Chapter 3 would be quite difficult to manufacture.

In the following, we will discuss the selection of the dimensions of the test specimen shown in Figure 4. There are quite a few constraints to be considered, some of them leading to conflicting requirements. It will be shown here that the best results are obtained when the length L_1 is approximately 50 mm and the thickness S_1 is a few mm. The width W_1 can be chosen more freely and is recommended here to be approximately 20 mm. The orientation shown in Figure 4 (with the longest edges being vertical) is a natural choice considering that the test specimen is being suspended from thermocouple wires; this orientation maximizes the distance from the suspension point to the center of gravity of the test specimen, which means that the dependence of the orientation on the exact location of the suspension point is rather weak. Thus, accuracy in the assembly of the test specimens will be less critical. As will be shown below, this orientation is also advantageous from the point of view of minimizing the contribution of convective heat transfer (cf. Section 4.3).
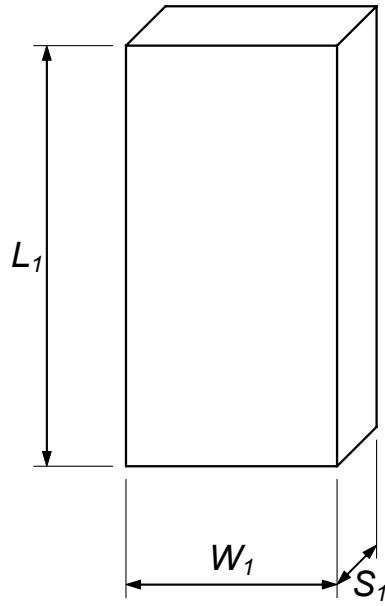
Figure 4. A schematic view of a test specimen (not in scale).

Assume that the slab shown in Figure 4 has been cut from a large plate. The slab has three pairs of opposing surfaces; one pair consists of the original surfaces of the plate and the other two pairs consist of new surfaces which were created when the test specimen was cut from the plate. It is quite possible that the emissivity of the original surface of the plate is different from the emissivity of the new surfaces; thus, the test specimen should be prepared in such a way that the new surfaces only constitute a small fraction of the total area of the test specimen. This point will be analyzed in the following.

In Figure 4, the total area of the test specimen is

$$A_{1,tot} \quad = \quad 2W_1 L_1 + 2W_1 S_1 + 2L_1 S_1 \tag{22}.$$

Now assume that the original surfaces of the plate form the surface facing the viewer and its opposing surface. The area of these two surfaces is

$$A_{1,o} \quad = \quad 2W_1 L_1 \tag{23}.$$

Thus, the fraction of the total surface area of the test specimen which consists of the original surface of the plate is obtained as

$$\gamma_o \quad = \quad \frac{A_{1,o}}{A_{1,tot}} \quad = \quad \frac{2W_1 L_1}{2W_1 L_1 + 2W_1 S_1 + 2L_1 S_1} \quad = \quad \frac{1}{1 + \dfrac{S_1}{L_1} + \dfrac{S_1}{W_1}} \tag{24}.$$

The results are illustrated in Figure 5, in which the value of γ_o is presented as a function of the thickness of the test specimen S_1 for the case of $L_1 = 50$ mm, $W_1 = 20$ mm. It can be seen that the value of γ_o decreases quite rapidly as the thickness of the test specimen increases. For instance, for a test specimen with a thickness of 5 mm, only 74 % of its surface area consists of the original surface of the material to be investigated; the rest consists of new surfaces, which were created when the test specimen was cut from the material. It is clear that there exists a potential source of uncertainty, and that the test specimens should not be made any thicker than what is necessary.

The uncertainty caused by the fact that the value of γ_o is less than unity can be expected to be particularly serious if materials with some special form of surface treatment are to be investigated. For such materials, the difference in emissivity between the treated surface and a freshly cut new surface might be quite significant. This class of materials also includes steel exposed to a fire, either a test fire in a laboratory or an accidental fire in an actual building. In such cases, other methods for the determination of emissivity might be preferable.
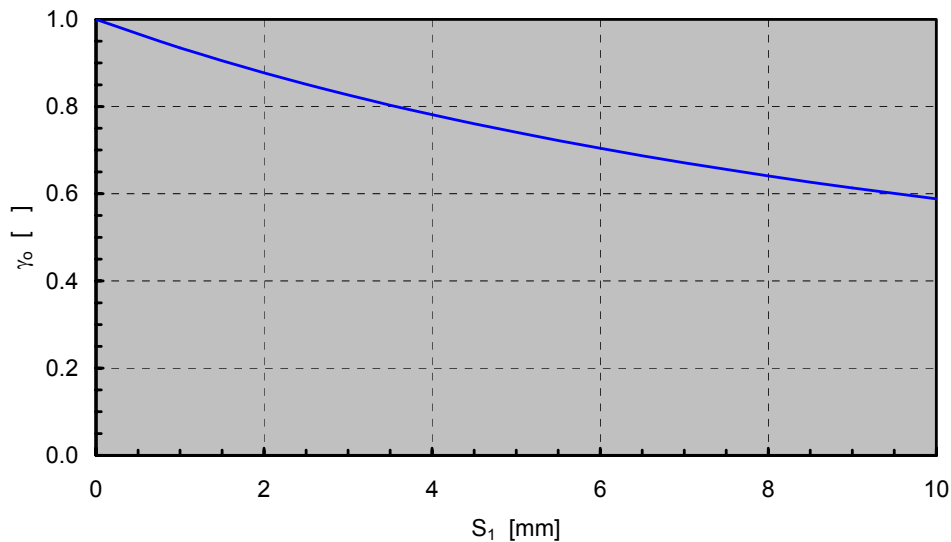

Figure 5. The fraction of the total surface area of the test specimen which consists of the original surface of the material to be studied for the case where the length and width of the test specimen are 50 mm and 20 mm, respectively.

Another factor that sets an upper limit to the thickness of the test specimen is the fact that the energy balance equation formulated in Section 3.3 was based on the assumption that the test specimen is at a uniform temperature throughout the test. In reality, there are variations of the internal temperature since a finite time is needed for the conduction of heat from the surface of the test specimen to the inner parts. A conservative estimate of the magnitude of the variations can be obtained in the manner which is explained below (see Figure 6 for nomenclature).

Consider a slab, for which the length and width are much larger than the thickness. Thus, the heat transfer problem is essentially one-dimensional. Let $\dot{q}_{tot}$ be the total heat flux from the surroundings to the surface of the test specimen and let λ_M be the thermal conductivity of the material of the test specimen. At the surface of the test specimen, the conduction heat flux to the interior of the test specimen must be equal to $\dot{q}_{tot}$; thus

$$\dot{q}_{tot} = \lambda_M \frac{dT_1}{dx} \approx \lambda_M \frac{\Delta T_{1,Int}}{\frac{1}{2}S_1} \tag{25}$$

from which we obtain

$$\Delta T_{1,Int} \approx \frac{\dot{q}_{tot}S_1}{2\lambda_M} \tag{26}.$$
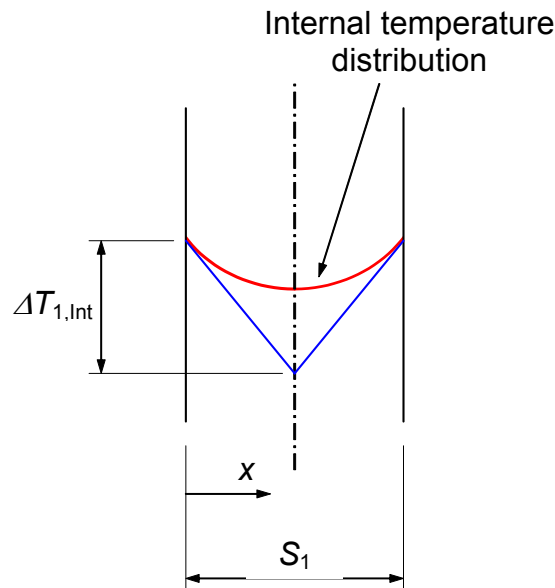

Figure 6. Estimation of the variations of the internal temperature of the test specimen.

For a furnace temperature of 600 ºC, the realistic upper limit for the value of $\dot{q}_{tot}$ can be estimated to be of the order of 30 kW/m^2. According to the VDI-Wärmeatlas (1984), the value of λ_M for stainless steel is approximately 20 W/(m·K). Thus, for a test specimen with a thickness of 5 mm, the value of $\Delta T_{1,Int}$ obtained from Equation (26) is of the order of 4 K. Although the estimate is believed to be conservative, it is clear that variations of this magnitude set the upper limit of the thickness of the test specimen at about 5 mm. If the experiments are to be carried out using a higher furnace temperature, then the thickness of the test specimen should be even smaller.

In addition to an upper limit, there is also a lower limit for the thickness of the test specimen. If the test specimen is too thin, it will heat up very rapidly in the furnace; the result is that the test specimen temperature will reach quite high values already during the settling period discussed in Section 4.3, and, consequently, no useful data will be obtained regarding the emissivity at low temperatures. The experience gained at VTT indicates that the thickness of the test specimen should be at least 2 mm. In the case of thinner materials, a sufficient thickness can be achieved with a multi-layer structure; this means that several layers of the original material are attached together to make a single test specimen of desired thickness. Care must be taken to ensure good contact between the layers in order to avoid excessive variations in the internal temperature of the test specimen.

In order to choose the test specimen length L_1, the convective heat transfer between the air in the furnace and the test specimen needs to be studied. VDI-Wärmeatlas (1984) gives the following equation to describe the heat transfer by natural convection between a fluid and a vertical plate suspended in the fluid:

$$\text{Nu} \quad = \quad \left\{ 0.825 + \frac{0.387\,\text{Ra}^{1/6}}{\left[1 + \left(\dfrac{0.492}{\text{Pr}}\right)^{9/16}\right]^{8/27}} \right\}^2 \tag{27}$$

which is quite similar to Equation (6). Thus, the computations can be carried out according to the procedure described in Section 3.2.3, except that the characteristic length of the test specimen is now L_1. Some results for the case where the furnace temperature is 700 ºC are shown in Figure 7. It can be seen that for a test specimen with a length of 5 cm, the value of the convective heat transfer coefficient is in the range 8…10 W/m^{2}K. For smaller test specimens, the value of the convective heat transfer coefficient is higher. Figure 7 suggests that in order to minimize the ratio of convective

heat transfer to radiative heat transfer, as was discussed in Section 4.3, the length of the test specimen should not be made smaller than approximately 5 cm.
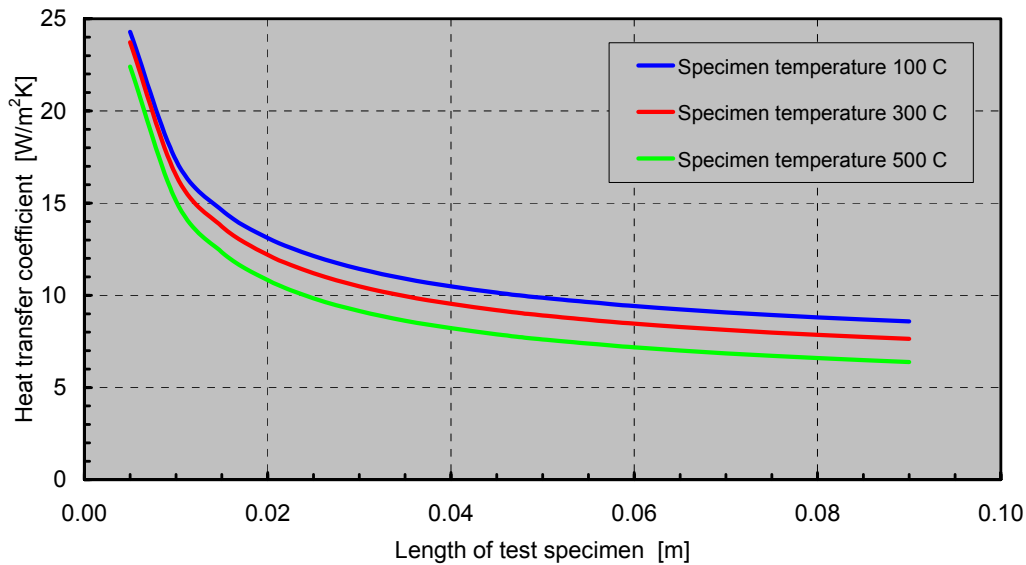

Figure 7. The convective heat transfer coefficient for natural convection between air and a vertical plate suspended in air. Air temperature 700 ℃.

At this point it is worth noting that the design of the experimental setup has now resulted in some deviations from the assumptions made during the development of the theoretical analysis in Chapter 3. Thus, the validity of the theoretical approach should be reassessed. From a mathematical point of view, Equation (1) is valid for any convex body located anywhere inside a larger cavity: as the basic equations of the net radiation method were solved, the only assumption that was made was that the configuration factor F_{1-1} was set equal to zero; in other words, it was assumed that the body cannot view itself. However, from a physical point of view the situation is more complex. If the shapes of the body and the cavity are non-spherical and if the body is located off the center of the cavity, then the radiative fluxes over the surfaces of the body and the cavity are non-uniform and the basic equations of the net radiation method are therefore not valid anymore. The normal procedure for handling such cases would be to divide the surfaces into smaller areas until the variations of the radiative fluxes over each area are not too large.

In this study, however, it would be very awkward to refine the analysis of heat radiation. Test specimens of different shapes and sizes are used, and the location and orientation of the test specimen varies in each experiment. Thus, the amount of work to analyze all cases would become very large. Furthermore, it seems obvious that the temperatures of the surfaces of the furnace chamber were also non-uniform during the experiments, and

Equations (1) and (2) can therefore only be expected to be approximately true. Nevertheless, we believe that they are sufficiently accurate for justifying the approach taken in this study.

As a conclusion of this section, it may be stated that the appropriate shape for the test specimens is a slab or a flat block having a thickness of the order of a few mm, a length of approximately 5 cm, and a width of a few cm. The thickness should be checked according to the thermal conductivity of the material to be investigated.

4.6 Temperature measurements

The temperatures of the test specimen and the furnace should be continuously recorded during the experiments. It is not very practical to measure the temperature distribution of the walls of the furnace chamber, and it is therefore assumed that after the settling period, the walls of the furnace chamber and the air inside the furnace chamber are at uniform temperature, and it will be sufficient to measure the temperature of the air in the furnace (cf. Section 4.3).

Any noise in the temperature measurements will make the interpretation of the data very difficult. This is mainly due to the fact that a time derivative of the temperature of the test specimen is needed in the computations (see Section 3.3). Thus, every attempt should be made to secure high quality of temperature measurements.

In order to be able to observe without delay the steep temperature changes occurring during the settling period, thermocouples with small-diameter wires should be used. Another advantage of small-diameter wires is that they will minimize the conduction of heat along the wires from the hot air in the furnace to the surface of the test specimen. It is well-known that thermocouple wires protruding from a surface act as heat transfer fins, and that the resulting heat flow may be quite significant (see, e.g. Chapman 1987). As the thermocouple wires are long and thin, they can be regarded as infinitely long, and the expression for the heat flow along one wire is (Chapman 1987)

$$\dot{Q}_{Cond,W} = \lambda_M \, m \, A \, (T_2 - T_1) \qquad (28)$$

where T_1 is the temperature of the test specimen, T_2 is the temperature of the air inside the furnace chamber, $A = \pi D^2 / 4$ is the cross-sectional area of the wire, λ_M is the thermal conductivity of the material of the wire, and parameter m is defined as

$$m = \sqrt{\frac{hP}{\lambda_M A}} \qquad (29)$$

where h is the heat transfer coefficient between air and the wire and $P = \pi D$ is the perimeter of the wire. By inserting Equation (29) into Equation (28), the heat flow along one wire becomes

$$\dot{Q}_{Cond,W} = \sqrt{hP\lambda_M A}(T_2 - T_1) = \frac{\pi}{2}\sqrt{h\lambda_M D^3}(T_2 - T_1) \qquad (30).$$

To illustrate Equation (30), the following numerical values are used: $D = 0.2$ mm, $T_1 = 20\,°C$, $T_2 = 700\,°C$, $h = 150$ W/m^{2}K (a fairly high value is used due to the small diameter of the wire), $\lambda_M = 20$ W/(m·K). The resulting heat flow along one wire is 0.17 W and the total heat flow along two wires is therefore 0.34 W. As was noted earlier, a realistic upper limit for the total heat flux to the test specimen is of the order of 30 kW/m^2 and the surface area of the test specimen is typically 20 cm^2; thus, the total heat flow to the test specimen can be estimated to be approximately 60 W. The conclusion is that the conduction of heat along the thermocouple wires is not significant in this example. However, it may be noted that the conduction heat flow along the wires increases quite rapidly with the wire diameter; for instance, using wires with a diameter of 0.5 mm would result in a conduction heat flow of 1.34 W which is already approaching the limit as to what can be regarded as acceptable.

4.7 Data logging

The requirements for the data logging system are not very strict. The number of channels is rather small, typically one temperature measurement for the test specimen and a few channels for monitoring the temperature of the furnace. The sampling frequency does not need to be higher than approximately 1 Hz.

4.8 Experimental procedure

In order to be able to use Equation (16) for evaluation of the emissivity, the surface area and mass of the test specimen must be known. It is good practice to measure these two quantities before the experiment. The mass of the test specimen may also be measured after the experiment; this provides a way to check whether significant physical or chemical changes of the test specimen occurred during the experiment, such as, e.g., oxidation.

4.9 Data processing

The data collected during the experiment are inserted into Equation (16) for evaluation of emissivity. Things that require attention are the evaluation of the time derivative of the test specimen temperature and the criteria for determining the beginning and end of the time period, during which useful data are obtained.

The time derivative of the test specimen temperature is difficult to evaluate since any noise in the temperature measurement will be amplified during the computation. Some type of smoothing of data will be quite necessary.

Useful data are obtained during a time period which is limited by two factors already discussed in Section 4.3:

- When the test specimen is inserted into the furnace chamber at the beginning of the experiment, the temperature distribution inside the furnace chamber is disturbed due to inflow of cold air; thus, useful data are not obtained until a uniform temperature distribution has been reached again. The period needed for reaching a uniform temperature distribution is called the settling period.

- As the temperature of the test specimen approaches the furnace temperature towards the end of the experiment, the heating rate of the test specimen slows down and the relative uncertainty in evaluating the dT_1/dt term in Equation (16) becomes very large.

The data processing scheme must have some way of deciding both the beginning and end of the period, during which useful data have been obtained.

5. Test materials

Three different test materials were used in the experiments. Test material TM-1 was cold-formed stainless steel cut from a 200 x 100 x 5 rectangular hollow section. The rectangular hollow section is shown in Figure 8. Test material TM-2 was cold-rolled stainless steel cut from a sheet with a thickness of 1.0 mm. Test material TM-3 was cold-rolled carbon steel cut from a sheet with a thickness of 1.5 mm. More details of the test materials are presented in Table 1.

Figure 8 shows that the appearance of the surface of the test material TM-1 is non-uniform with some glossy stripes between larger matt areas. This observation will be further discussed in Sections 7.1.3, 7.2 and 8.1.

Figure 8. Test material TM-1 (cold-formed 200 x 100 x 5 rectangular hollow section made of stainless steel).

Table 1. Test materials employed in the study.

|	Material	Thickness	Surface finish	
			Code	Description
TM-1	Stainless steel EN 1.4301 (ASTM 304)	5.0 mm		Lightly brushed surface
TM-2	Stainless steel EN 1.4301 (ASTM 304)	1.0 mm	2B	Cold-rolled, annealed and pickled and lightly rolled on polished rolls
TM-3	Carbon steel EN 10130 DC01 (ASTM A366)	1.5 mm	Am	Normal (ASTM Class 2 matte)

6. Tests using the new method

6.1 Equipment and procedure

6.1.1 Test furnace

A Labotherm L9/S electrically heated laboratory furnace was used in the experiments. The nominal maximum temperature of the furnace is 1100 ºC. Heating elements are located above the ceiling and below the roof of the furnace chamber. The dimensions of the furnace chamber are: width 240 mm, depth 250 mm, height 170 mm, which results in a surface area of 0.29 m^2.

The furnace is shown in Figure 9. The wire net structure inside the furnace chamber is a holder for the thermocouples used for the measurement of the air temperature. The temperature measurement system is described in Section 6.1.3.
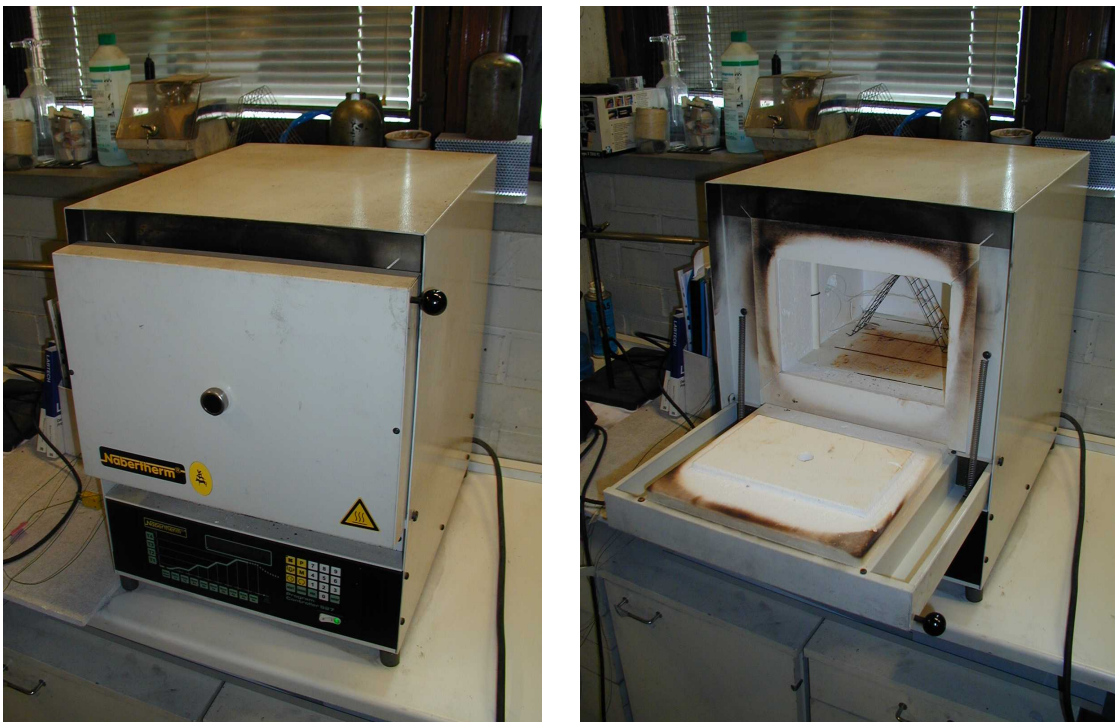
Figure 9. Labotherm L9/S laboratory furnace used in the experiments.

6.1.2 Test specimens and specimen holders

Test specimens of two different sizes were used in the VTT tests. Majority of test specimens had a length of approximately 50 mm and a width of approximately 20 mm. This size had been found to be optimal with regard to the considerations presented in Section 4.5. Some test specimens with a length of approximately 25 mm were also made. The purpose of the smaller test specimens was to produce data that could be used to check the validity of the theoretical approach. As was noted in Section 4.5, the value of the convective heat transfer coefficient was expected to be significantly higher for the smaller test specimens than for larger test specimens; thus, if the emissivity values computed from the experimental results were independent of the size of the test specimens, then the treatment of convection heat transfer would seem to be correct, and, on the other hand, if the emissivity values computed from the experimental results exhibited a systematic dependence on the size of the test specimens, then the treatment of the convection heat transfer would have to be put in doubt.

As regards the thickness of the test specimens, a decision had to be made on whether to make single-layer or multi-layer test specimens. The decision was related to the analysis on the thermal behavior of the test specimens, as was discussed in Section 4.5. The thickness of test material TM-1 was 5 mm; this was within the optimal range, so the test specimens could be of the single-layer type. The thicknesses of test material TM-2 and test material TM-3 were 1 mm and 1.5 mm, respectively; these values were too small and double-layer test specimens were therefore prepared. The methods of preparation are described below.

Before the experiments, all test specimens were weighted and their dimensions were measured with a slide gage. The surface areas were computed from the dimensions by assuming a rectangular shape.
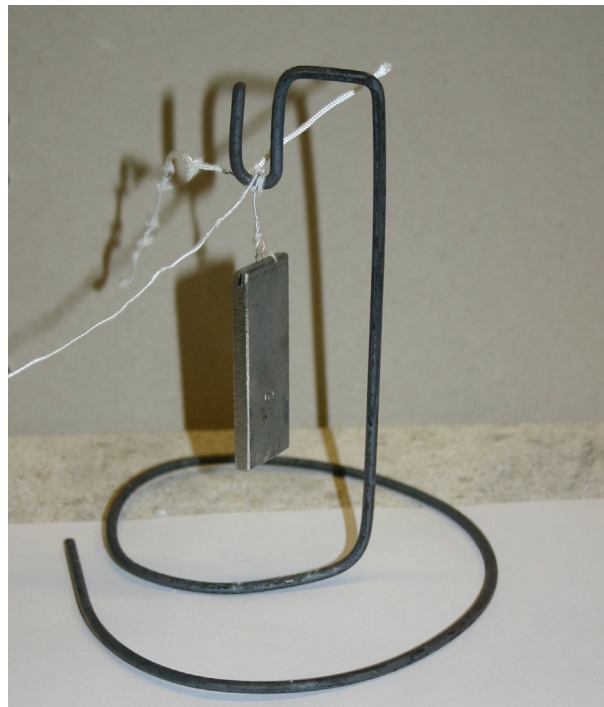
Seven test specimens were made from test material TM-1: five large test specimens and two small ones. Slabs of suitable size were first sawed from the material. A rectangular groove with a depth of a few mm was then sawed to one end of the test specimen, as shown in Figure 10. A thermocouple for measuring the temperature of the test specimen was inserted into the groove and the sides of the groove were tightly pressed around the thermocouple using a screw press. The thermocouple was also used to suspend the test specimen from a specimen holder made of stainless steel wire. A photograph of a test specimen made from test material TM-1 and a specimen holder is shown in Figure 11.

Two different specimen holders were employed in the test: a larger one and a smaller one. The specimen holder shown in Figure 11 is the larger one. The larger specimen

holder was much more convenient in use, since it was more stable than the smaller one. No differences were observed in the results obtained with different specimen holders.
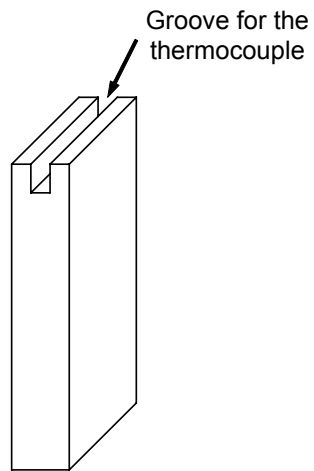
Figure 10. A schematic view of test specimens made from test material TM-1 (not in scale).

Figure 11. A photograph of test specimen TM-1-5 hanging from the specimen holder on a thermocouple.

Eight test specimens were made from test material TM-2: five large test specimens and three small ones. Two methods were used for achieving the double-layer structure. The first three test specimens were made using method (a) and the last five test specimens were made using method (b).

(a) A rectangular piece was first cut from the sheet. The size of the piece was twice the size of the test specimen. Then the sheet was folded, a thermocouple was inserted between the halves, and the halves were pressed together.

(b) Two rectangular pieces were first cut from the sheet. The sizes of the pieces were equal to the size of the test specimen. Then the pieces were set against each other, two of the corners were electrically welded together, a thermocouple was inserted between the pieces, and the last two corners were welded together.

Six test specimens were made from test material TM-3. They were all large and made using method (b) described above. A photograph of a test specimen made from test material TM-3 is shown in Figure 12.

Figure 12. A photograph of test specimen TM-3-6 hanging from the specimen holder on a thermocouple. Color changes in the corners of the test specimen are due to welding.

6.1.3 Temperature measurements

The temperatures of the test specimens and of the air inside the furnace were measured using K type thermocouples with a wire diameter of 0.20 mm. Three thermocouples were used for furnace temperature measurements. They were positioned at heights of 20 mm, 70 mm and 120 mm above the floor of the furnace chamber by using a holder made of stainless steel wire net. The arrangement of the temperature measurement is shown in Figure 13.

The thermocouple wires were originally surrounded by an insulation which could only withstand a temperature of 400 ºC. When exposed to higher temperatures, the insulation material ignited and burned leaving a solid white residue, which remained around the thermocouple wires and resembled the original insulation in shape. During the burning of the insulation, the signals produced by the thermocouples oscillated wildly and no useful data could be obtained. However, it had been found during earlier work that the thermocouples still seemed to work after the burning had ceased and could be used for the measurement of much higher temperatures than those presented in the original specification. Thus, all experiments were carried out using "pre-burned" thermocouples.

Figure 13. The thermocouples and thermocouple holder for the measurement of the air temperature inside the furnace chamber.

To assess the accuracy of temperature measurements, three "pre-burned" thermocouples were tested in a calibration furnace for the temperature range 100…700 ºC using steps of 100 ºC. All three thermocouples gave very similar results: at 100 ºC, the measured temperatures were approximately 1 ºC higher than the actual temperature; at 200 ºC, the measured temperatures were approximately 1 ºC lower than the actual temperature; and as the temperature further increased, the deviations slowly increased in magnitude until at 700 ºC, the measured temperatures were approximately 3…4 ºC lower than the actual temperature. In the higher temperatures, the observed deviations were slightly larger than those specified for the IEC tolerance class I, but the accuracy of the temperature measurements was nevertheless regarded as acceptable.

In most of the experiments, the temperature measurement system performed quite well. In some experiments, however, the thermocouples failed and limited or no data could be collected. In some other experiments, the signals were excessively noisy, and special methods had to be employed in the analysis of data. The analysis methods are described in Section 6.1.6.

Figure 14 shows the temperature distribution of the air inside the furnace chamber during the disturbance caused by opening the furnace door for 5 seconds. In the experiments, 4…5 seconds were normally needed for the insertion of the test specimen, but in this case no test specimen was inserted into the furnace. It can be seen that the length of the settling period was approximately 20 seconds.
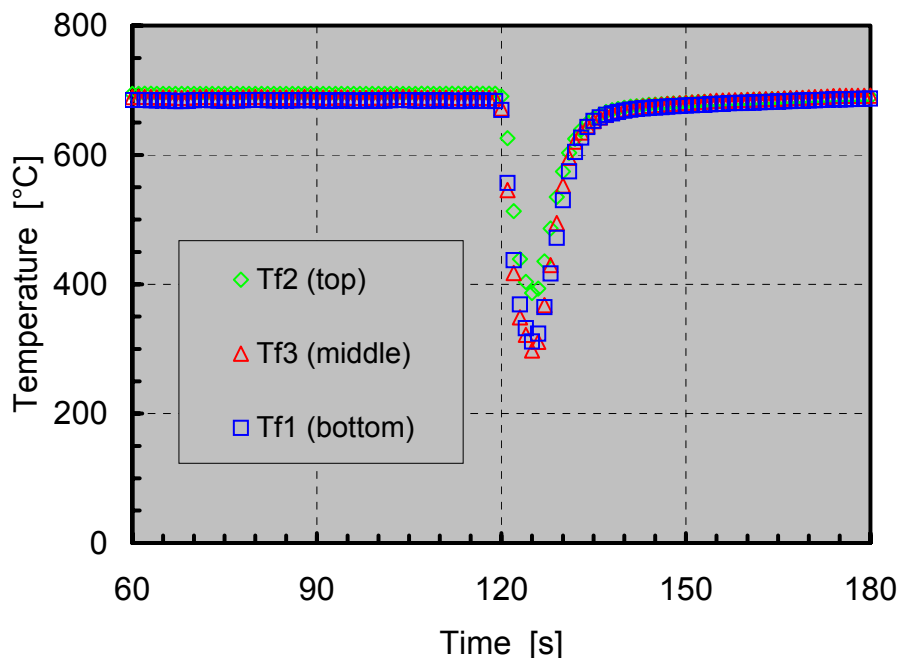

Figure 14. Measurement of air temperature distribution inside the furnace chamber during the disturbance caused by opening of the furnace door for 5 seconds.

6.1.4 Data logging

A microcomputer-controlled datalogger was used to record the temperatures of the test specimen (one channel) and the air inside the furnace chamber (three channels) at intervals of one second. The data were stored as ASCII files for further processing.

6.1.5 Experimental procedure

The experiments were started by slowly heating the furnace to the desired temperature. In the experiments reported here, furnace temperatures in the range 600…700 ℃ were employed. During this stage, the test specimens were kept at room temperature.

The test specimens had to be suspended from the specimen holder before they could be inserted into the furnace. The thermocouple used for measuring the temperature of the test specimen was attached to the specimen holder with a short piece of pre-burned thermocouple wire (cf. Section 6.1.3). The arrangement can be seen in Figure 12.

After the furnace had been at least one hour at the setpoint temperature, data logging was started. After typically two minutes of baseline recording, the furnace door was opened, the test specimen and specimen holder were swiftly inserted, and the furnace door was closed again. In the experiments, all this normally took 4…5 seconds. When the temperature of the test specimen started to approach the furnace temperature (this normally occurred after a couple of minutes), the furnace door was opened again and the test specimen and specimen holder were removed from the furnace. Finally, data logging was terminated.

Some test specimens were photographed before and after the experiments using a digital camera.

6.1.6 Data processing

The ASCII files produced by the data logging system were transferred to a Microsoft Excel spreadsheet for further processing. The Excel spreadsheet had been constructed to solve Equation (16) and to carry out uncertainty analysis for each instant of time and to prepare the necessary plots of the results.

Two different procedures were employed. Most of the data were analyzed using what will be called the standard procedure. This procedure seemed to work reasonably well in cases where the temperature data were sufficiently smooth. In some experiments,

however, the temperature measurements were contaminated by low-frequency noise of unknown origin and additional smoothing had to be introduced. Both the standard procedure and the modified procedure will be illustrated below.

The input data for Equation (16) were obtained as follows:

1. Standard procedure

(a) The mass of each test specimen was weighted during the fabricating process.

(b) The linear dimensions of each test specimen were measured using a slide gage, and the surface area was then computed using Equation (22).

(c) The specific heats of the tested materials were assumed to be linear functions of temperature. For ASTM 304 stainless steel (test materials TM-1 and TM-2), a straight line was fitted to the data presented by Lewis (1977). For carbon steel (test material TM-3), a straight line was fitted to the third-degree polynomial presented in Part 1.2 of the draft version of Eurocode 3 (2002).

(d) The temperature of the test specimen was measured using a thermocouple embedded into the test specimen (see Section 6.1.2 for details).

(e) The temperature of the furnace was taken to be the average value of the three thermocouples positioned at different heights in the furnace chamber (see Section 6.1.3).

(f) The time derivative of the test specimen temperature dT_1/dt was computed in the following manner. Firstly, a nine-point average temperature was computed for each instant of time (the nine points consisted of the time being considered and the nearest four measurements before and after the time being considered). After that, the time derivative at $t = t_i$ was obtained from the normal center difference formula $dT_1/dt = (T_{1,i+1} - T_{1,i-1})/(2\Delta t)$.

(g) The convective heat transfer coefficient between the test specimen and the air inside the furnace chamber was computed using Equations (27) and (7)–(10). The thermal properties of the air were taken at the average temperature between the air and the test specimen $\overline{T} = (T_1 + T_2)/2$. For the computation of the thermal properties, the equations presented by Laine (1998) were employed.

45

2. Modified procedure (additional 60 s averaging)

- As the standard procedure, except that all temperature values were taken as 60 s sliding average values.

Good quality temperature data and the emissivity values obtained using the standard procedure are illustrated in Figure 15 and Figure 16. The results appear to be quite reasonable. However, the standard procedure appears to be nearly useless if low-quality data contaminated by low-frequency noise are analyzed. This is illustrated in Figure 17 and Figure 18. It can be seen that the temperature fluctuations are propagated into the computed values of emissivity with disastrous results. To solve this problem, the modified procedure was applied in cases with low quality temperature data.

It was important to ensure that the results would not be distorted by the additional 60 s averaging carried out as part of the modified procedure. Examples of the effect of the additional 60 s averaging are presented in Figure 19 and in Figure 21. It can be seen that the temperature changes which occur as the test specimen is inserted into and removed from the furnace have become much more gradual. Comparisons of emissivity values computed using the standard procedure with emissivity values computed using the modified procedure are presented in Figure 20 and in Figure 22. The additional 60 s averaging appears to produce the desired effect: the results are smoother than the results obtained using the standard procedure but otherwise there is no difference.

Results from some other tests indicated, however, that the additional 60 s averaging is likely to distort the results if the temperature dependence of the emissivity is stronger than for test material TM-1. Thus, the 60 s averaging was only used for processing the results of November 2004 tests of test material TM-1.

Finally, one has to choose the starting point and end point for data processing. The starting point for data processing shall be at the end of the settling period, that is, at the point where the furnace temperature has become sufficiently uniform to allow the use of Equation (16) for processing of data. In this study, the starting point was chosen to be the instant of time when the furnace temperature had been restored to within 20 ºC of the setpoint value. The end point for data processing shall be at the point when the rate of change of the temperature of the test specimen has slowed down to such an extent that the relative uncertainty in the dT_1/dt term becomes too large. In this study, the end point was chosen to be the instant of time when the temperature of the test specimen had reached a value which was 100 ºC lower than the setpoint value of the furnace. It should be noted that the selection of the starting point and the end point are quite subjective.
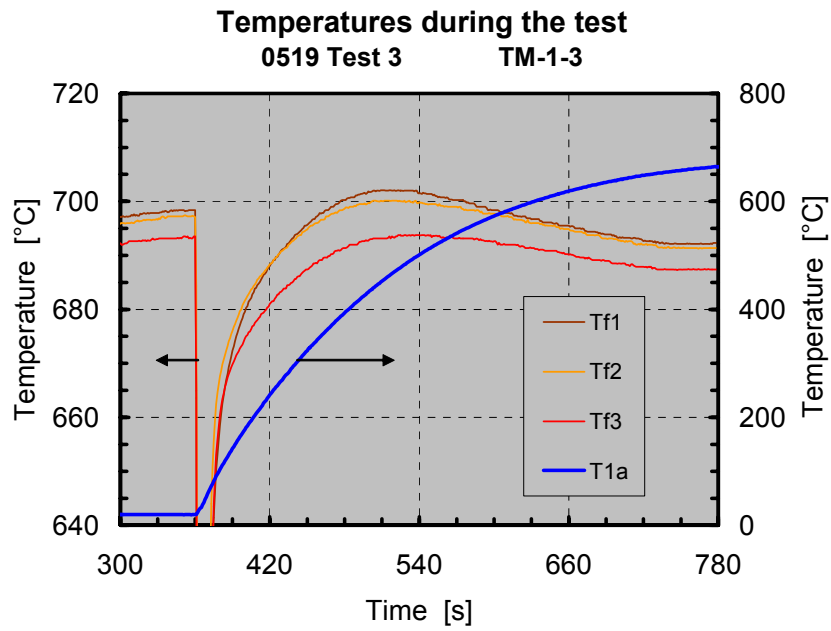
Figure 15. An example of good quality temperature data. Test specimen TM-1-3 measured on 19 May 2004.
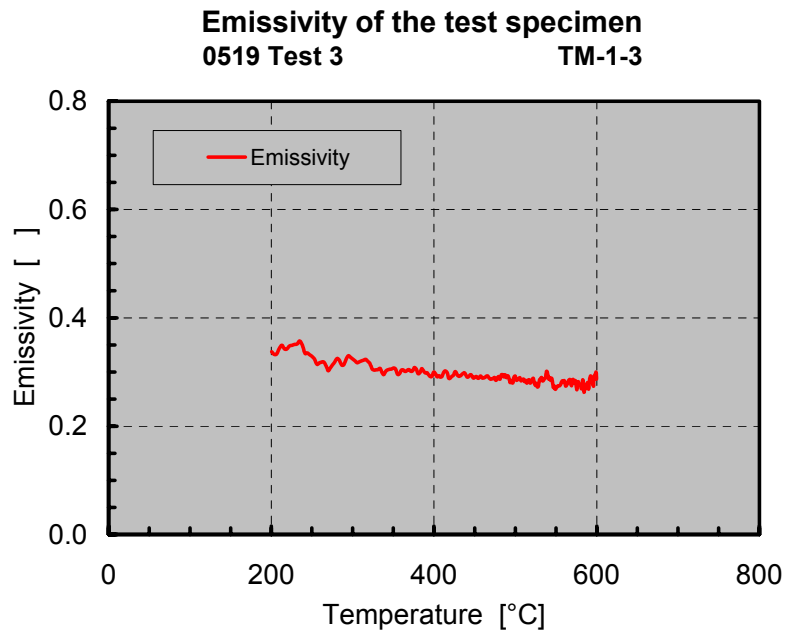

Figure 16. An example of good quality results obtained using the standard procedure. Input data from Figure 15 (test specimen TM-1-3 measured on 19 May 2004).
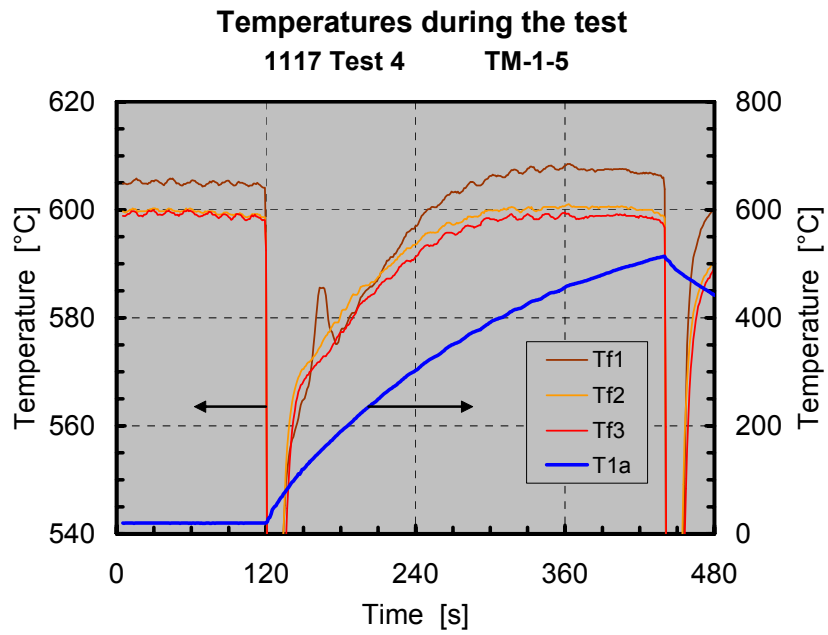
Figure 17. An example of poor quality temperature data. Test specimen TM-1-5 measured on 17 Nov 2004.
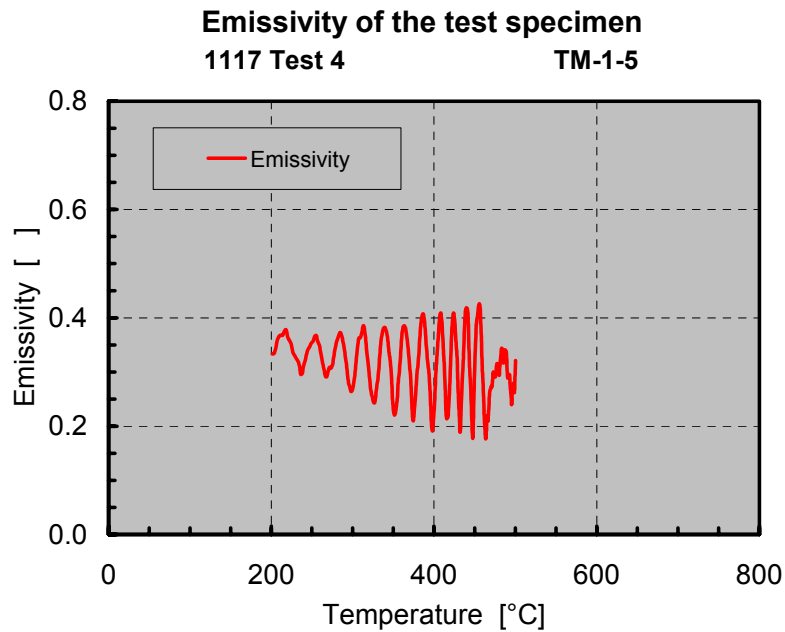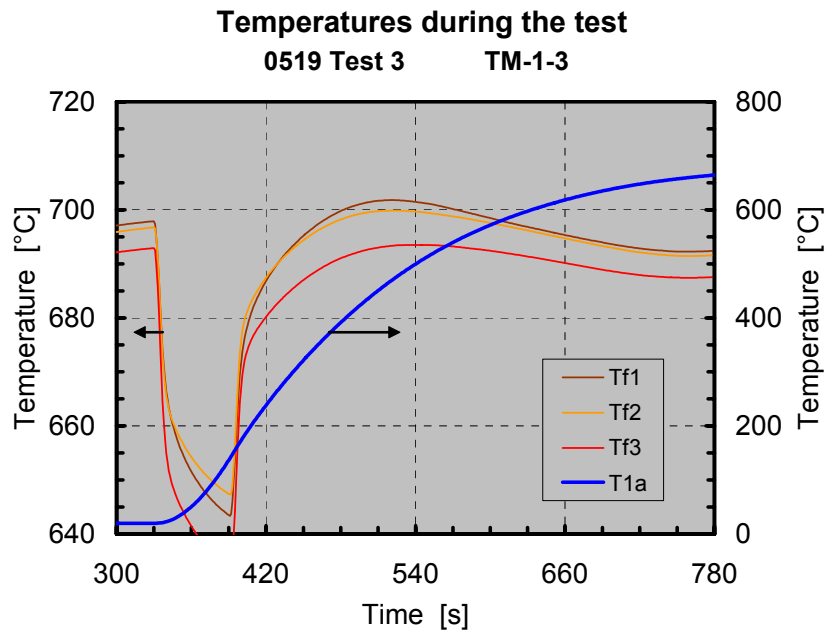

Figure 18. An example of poor quality results obtained using the standard procedure. Input data from Figure 17 (test specimen TM-1-5 measured on 17 Nov 2004).

Figure 19. The temperature data shown in Figure 15 after additional 60 s averaging has been applied.
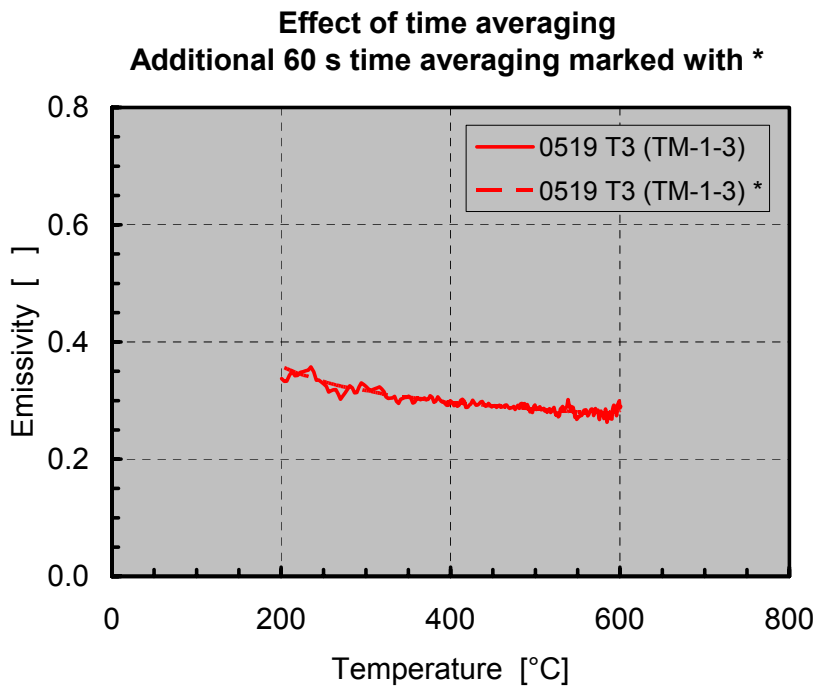
Figure 20. Comparison of results obtained using the standard procedure with results obtained using the modified procedure (additional 60 s averaging). Input data from Figure 15 and Figure 19 (test specimen TM-1-3 measured on 19 May 2004).
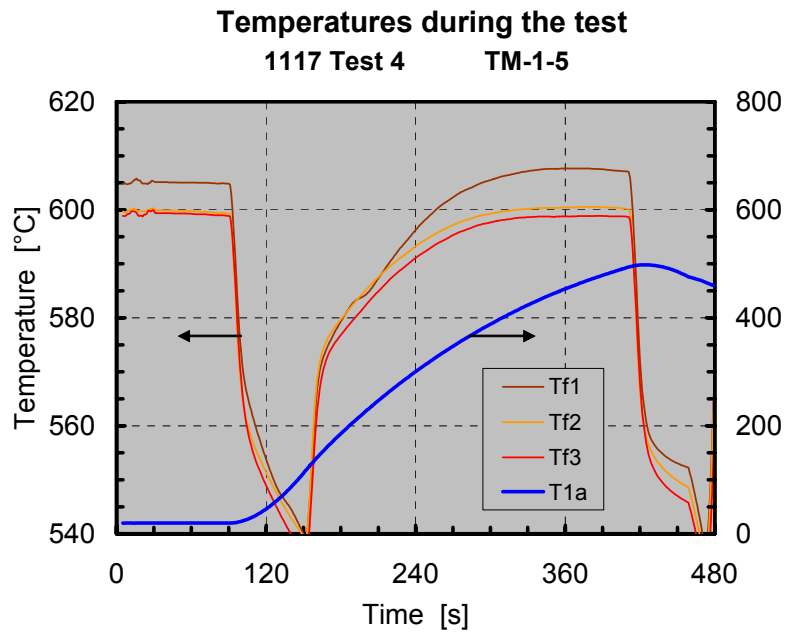
Figure 21. The temperature data shown in Figure 17 after additional 60 s averaging has been applied.
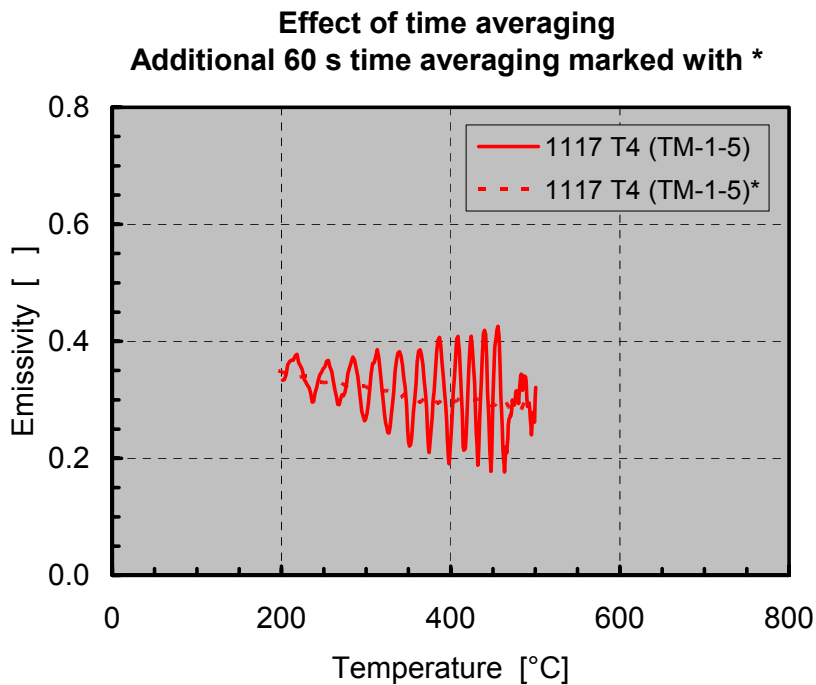
Figure 22. Comparison of results obtained using the standard procedure with results obtained using the modified procedure (additional 60 s averaging). Input data from Figure 17 and Figure 21 (test specimen TM-1-5 measured on 17 Nov 2004).

6.1.7 Uncertainty analysis

The method developed in this study is based on computing ε, the value of emissivity, as a function of the measured values of the quantities on the right-hand side of Equation (16). Uncertainty analysis provides a tool to estimate $u(\varepsilon)$, the uncertainty of the value of emissivity, as a function of the measured values and uncertainties of the quantities on the right-hand side of Equation (16). In the language of uncertainty analysis, ε is the measurand, $u(\varepsilon)$ is the uncertainty of measurement, and the quantities on the right-hand side of Equation (16) are input quantities.

The uncertainty of measurement is a parameter that characterizes the dispersion of the values that could reasonably be attributed to the measurand. If the probability distributions of the uncertainties of the input quantities are known, then it should be possible, at least in principle, to formally derive the probability distribution of the uncertainty of measurement. In such cases, a fully quantitative interpretation of the uncertainty of measurement can be presented; e.g., a 95 % confidence interval can be computed. However, in many cases the probability distributions of the input quantities are not known. In such cases, the interpretation of the uncertainty of measurement will unavoidably remain semi-quantitative; this is also the case here. Thus, while a strictly formal procedure is applied to analyze the propagation of uncertainty from the input quantities to the measurand, the exact interpretation is still missing. We are merely making statements of the type: "If the uncertainty of the value of the test specimen temperature can reasonably be expected to be smaller than 4 K etc., then the uncertainty of the value of emissivity can reasonably be expected to be less than ±20 %." No attempt will be made to define what exactly we mean here by "reasonably".

The uncertainty analysis of this study was performed according to the procedure outlined in the document EAL-R2 (1997). For a relationship of the type

$$y \;=\; x_1 + x_2 \tag{31}$$

the uncertainty associated with the estimate of y was taken to be

$$u(y) \;=\; \sqrt{[u(x_1)]^2 + [u(x_2)]^2} \tag{32}$$

and for a relationship of the type

$$y \;=\; x_1^m x_2^n \tag{33}$$

the relative uncertainty associated with the estimate of y was taken to be

$$\frac{u(y)}{y} \ = \ \sqrt{m^2\left[\frac{u(x_1)}{x_1}\right]^2 + n^2\left[\frac{u(x_2)}{x_2}\right]^2}$$

<div align="right">(34).</div>

Equations (32) and (34) were then applied step by step to each term in Equation (16). The computations were incorporated into the Microsoft Excel spreadsheet used in analyzing the data, and an estimate of the uncertainty of the emissivity value was therefore automatically produced for each instant of time.

Estimates of the uncertainties of the input quantities are given in Table 2. The major sources of uncertainty were found to be the measurement of the furnace temperature, the estimation of the time derivative of the test specimen temperature, and the estimation of the convective heat transfer coefficient.

An example of the uncertainty associated with the emissivity values determined in Test 3 of 19 May 2004 is shown in Figure 24. This experiment was already used to illustrate the data and results in the previous section. The uncertainties are found to be of the order of ±20 % for most of the temperature range. At the highest temperatures the uncertainty starts to increase and is of the order of ±30 % at 600 ºC. The reason is that as the temperature of the test specimen starts to approach the furnace temperature, the time derivative of the test specimen temperature becomes quite small, and therefore the relative uncertainty of the time derivative of the test specimen temperature becomes the dominating factor in the uncertainty budget.

The uncertainties in other experiments with test material TM-1 and in the experiments with the other two test materials were of similar magnitude.

Table 2. Estimated uncertainties of the input quantities of Equation (16).

Quantity	Estimated uncertainty	Notes
T_1	4 K	Estimate based on IEC specifications and calibration tests (see Section 6.1.3). Non-uniformity of the test specimen temperature also considered (see Section 4.5).
T_2	20 K	Furnace temperature measurements are not expected to be very accurate (see discussions in Section 4.3 and the observed vertical temperature gradient in, e.g., Figure 15).
dT_1/dt	0.2 K/s	Estimated from the fluctuations observed in the behavior of the time derivative computed using the center difference formula and nine-point average values of test specimen temperature (see Figure 23).
m_1	0.01 g	Based on the accuracy of the balance.
A_1	0.4 cm^2	Based on the accuracy of the slide gage.
c_{p1}	20 J/kgK	Based on deviations between the actual dependence of specific heat on temperature and the straight-line fit used in computations.
h_{Conv}	1 W/m^{2}K	Based on estimated uncertainty associated with convection heat transfer equations.
σ	5·10^{-11} W/m^{2}K^4	The value of the Stefan-Boltzmann constant was used with three significant digits.
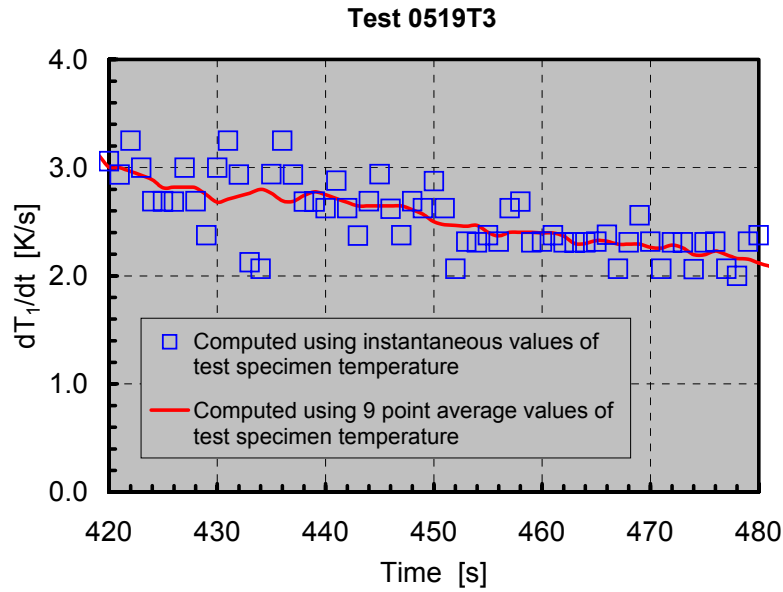
Figure 23. An example of the evolution of the time derivative of the test specimen temperature. For the time derivative computed using 9 point average values of test specimen temperature, the fluctuations about the mean are estimated to be 0.2 K/s
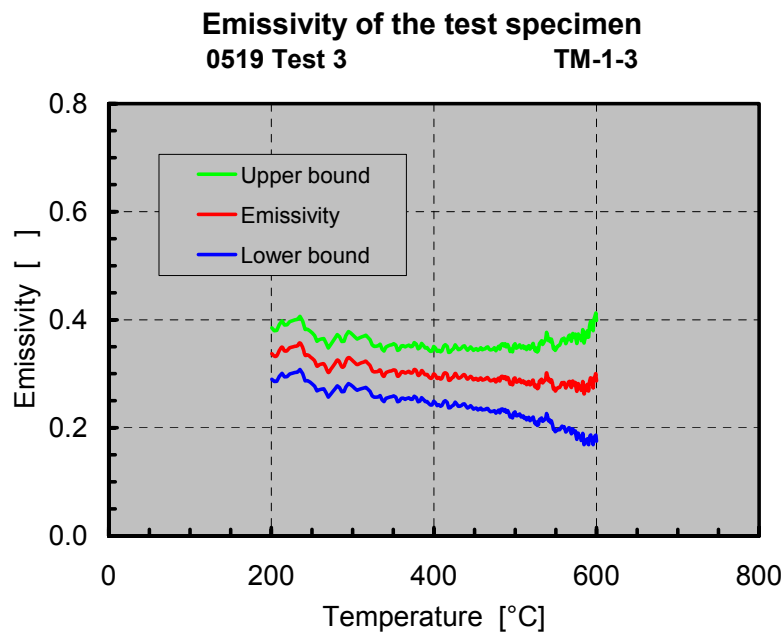
Figure 24. The results from Test 3 of 19 May 2004 (Test specimen TM-1-3) shown with estimates of the uncertainty interval.

6.2 Checking the consistency of the results

This section contains a summary of the experiments which were carried out to test the validity of the new method. The first subsection deals with the repeatability of the results. The two other subsections deal with the possible influence of the furnace temperature and the size of the test specimen on the results. These two variables can be controlled by the experimentalist and can therefore be used as system checks. Naturally, it is expected that neither the furnace temperature nor the size of the test specimen should have any influence on the results.

6.2.1 Repeatability

Results of repeatability tests are shown in Figures 25–27. In all three cases, the repeatability appears to be very good.
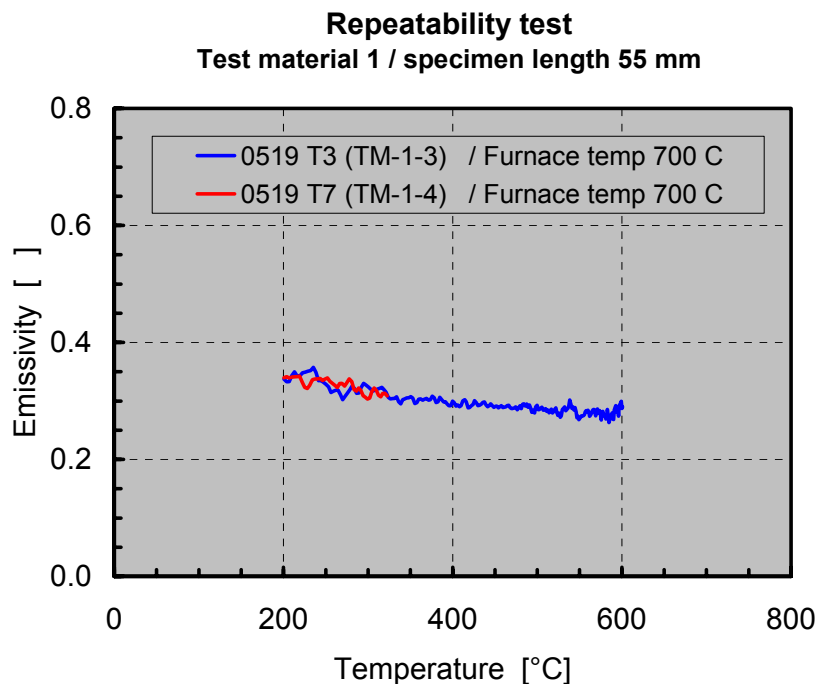
Figure 25. Repeatability test for test material TM-1 on 19 May 2004. The measurement of the temperature of test specimen TM-1-4 failed during the experiment, and the curve is therefore terminated at 300 ℃.

55
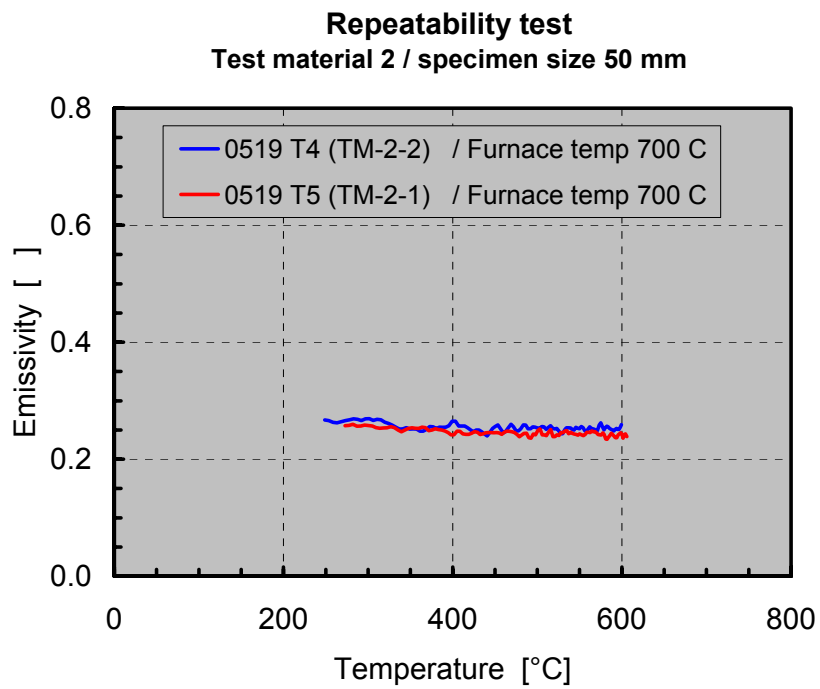
Figure 26. Repeatability test for test material TM-2 on 19 May 2004.
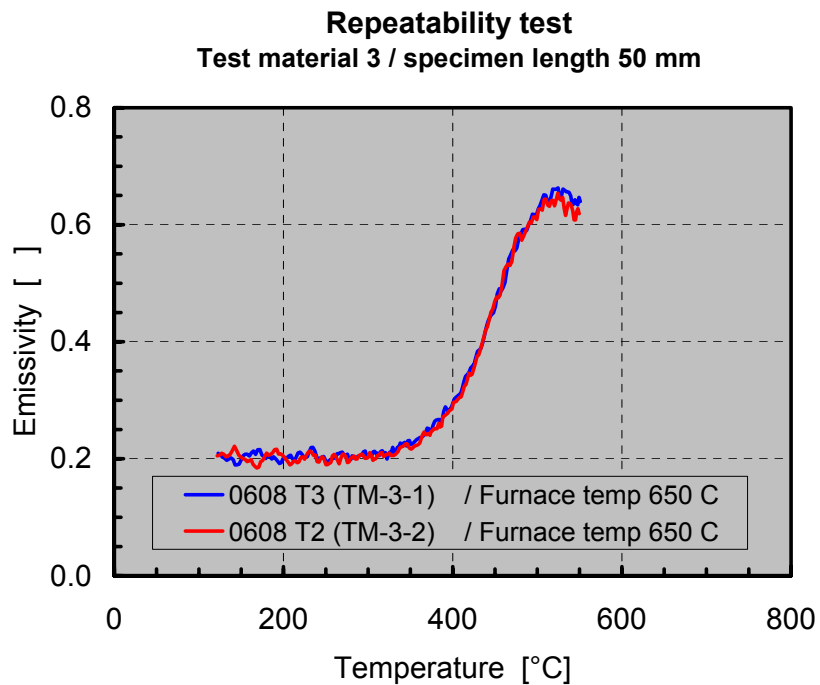
Figure 27. Repeatability test for test material TM-3 on 8 June 2004.

6.2.2 Effect of furnace temperature

The furnace temperature was varied within the range 600…700 ºC in the experiments. The temperature range had to be relatively narrow in view of the considerations presented in Section 4.3. However, the dependence of the thermal radiation on the 4th power of temperature means that even within this temperature range the relative contributions of thermal radiation and convection to heat transfer change quite significantly (cf. Figure 2).

The effect of furnace temperature on the results is presented in Figures 28–30. No systematic trends can be observed, which appears to confirm the validity of the approach. For test material TM-1, the lowest emissivity values were obtained at a furnace temperature of 650 ºC, which is in the middle of the temperature range studied in the tests. It must be pointed out, however, that in the case of test materials TM-2 and TM-3 the furnace temperature was only varied within a very narrow range.
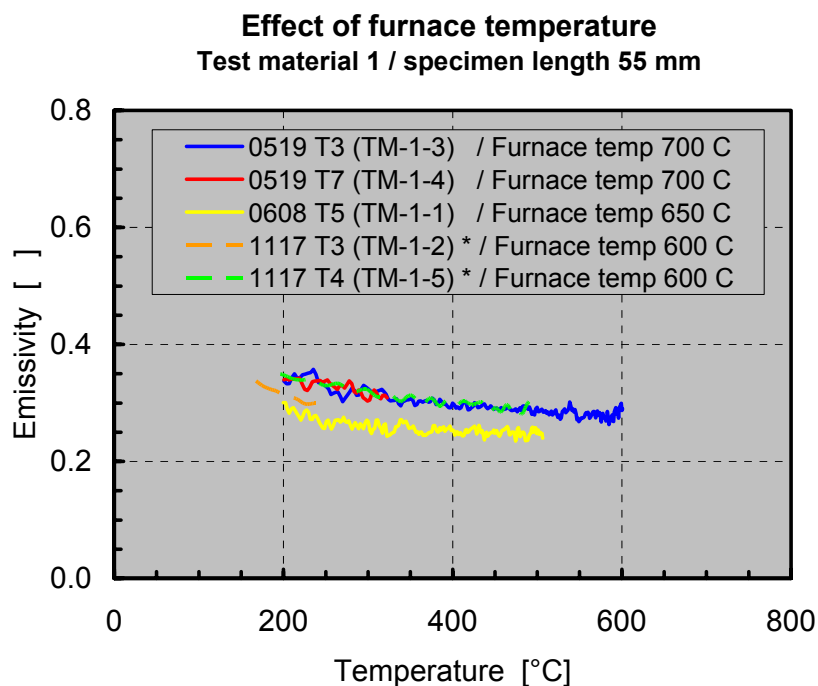
Figure 28. The effect of furnace temperature in experiments with test material TM-1.
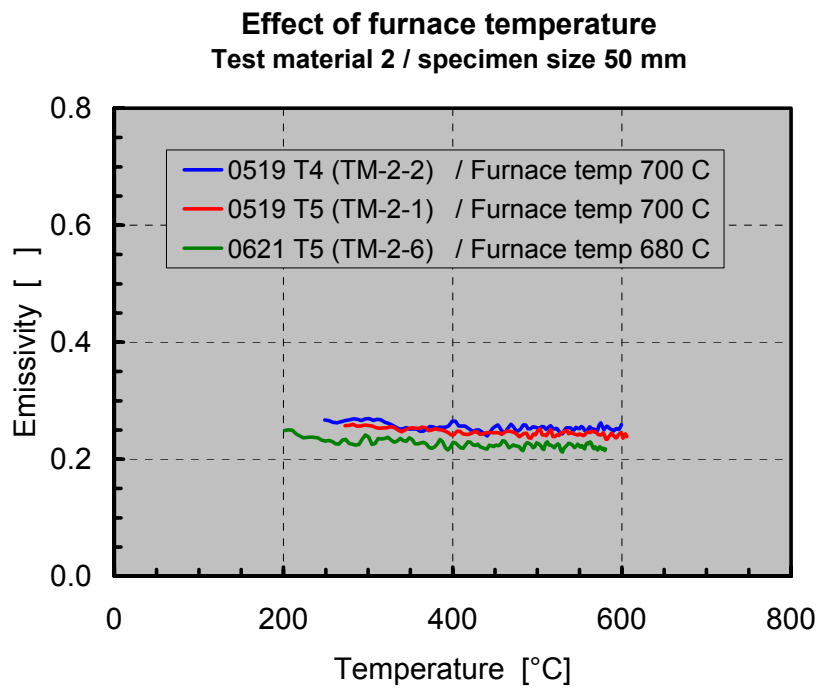
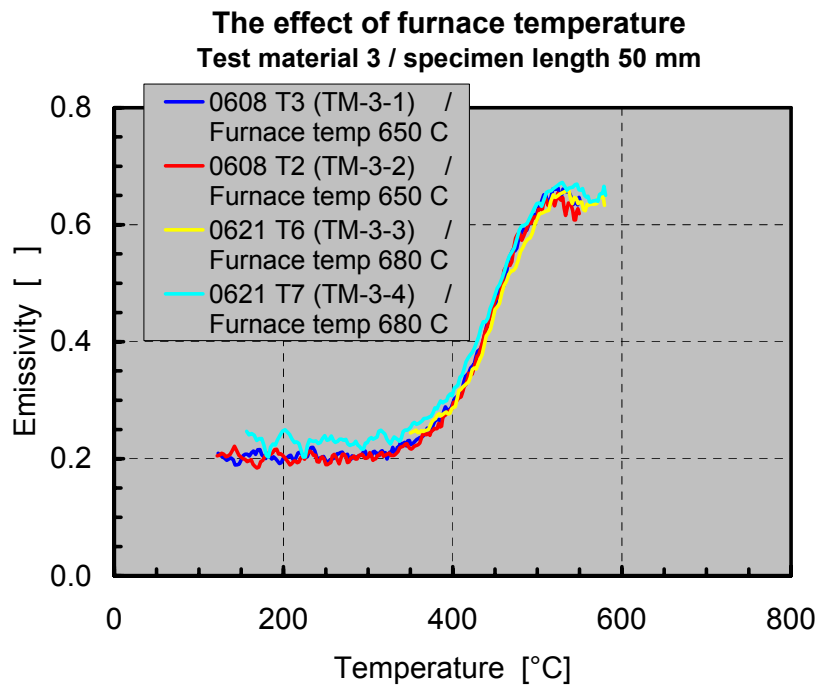*Figure 29. The effect of furnace temperature in experiments with test material TM-2.*

Figure 30. The effect of furnace temperature in experiments with test material TM-3.

6.2.3 Effect of the size of the test specimen

As was described in Section 6.1.2, majority of the test specimens had a length of approximately 50 mm but some test specimens with a length of approximately 25 mm were also made. Such a difference in length was expected to result in quite considerable variations in the value of the convective heat transfer coefficient (cf. Section 4.5). Thus, the size of the test specimen could be used to check the validity of the approach.

The effect of the size of the test specimen is shown in Figure 31 for test material TM-1 and in Figure 32 for test material TM-2. No systematic trends can be observed, which appears to confirm the validity of the approach. For test material TM-3, all test specimens were of the same size.
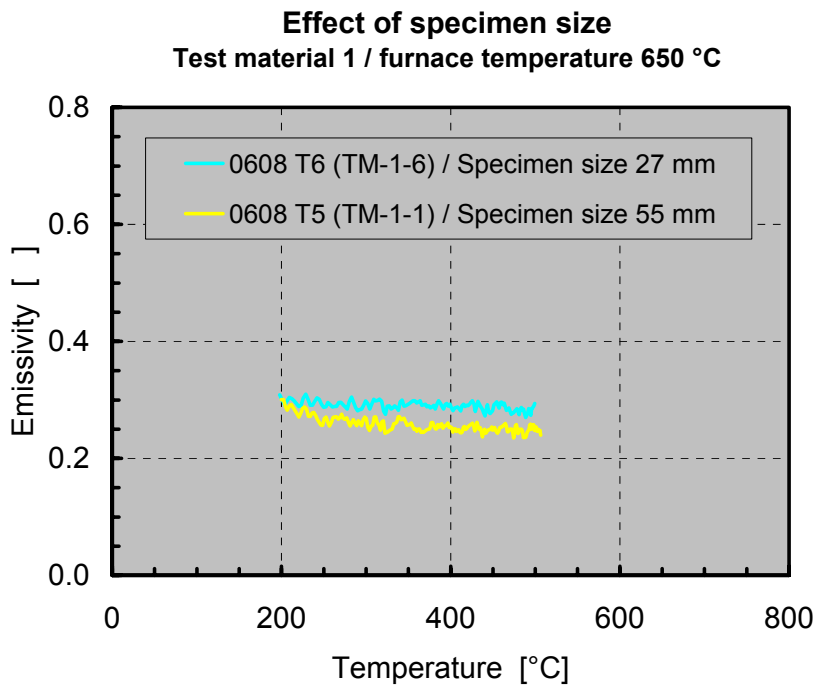
Figure 31. The effect of the size of the test specimen on the emissivity values for test material TM-1.
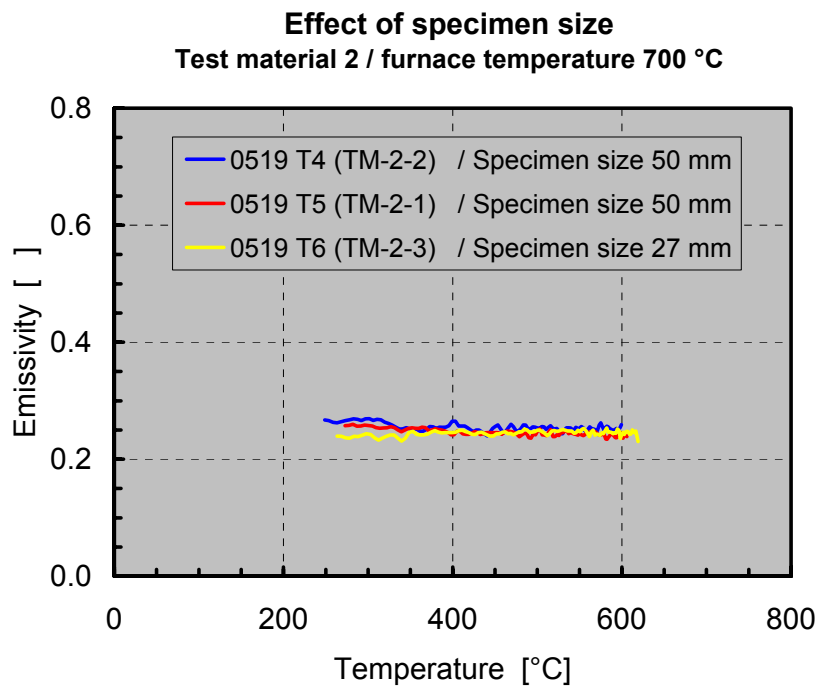
Figure 32. The effect of the size of the test specimen on the emissivity values for test material TM-2.

6.3 Summary of actual results for the test materials

6.3.1 Test material TM-1

A summary of all results obtained for test material TM-1 using the new method is presented in Figure 33. Due to the problems discussed in Section 4.3, emissivity was only obtained for temperature range 200…600 ºC. Within this range, the emissivity of test material TM-1 appears to be a weakly decreasing function of temperature.
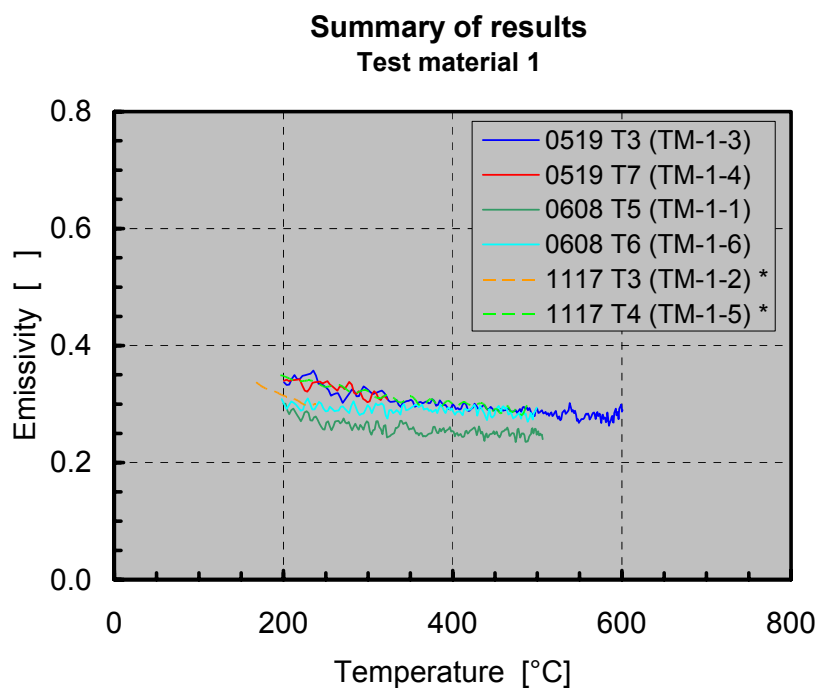
Figure 33. Summary of all results obtained for test material TM-1 using the new method. Solid lines indicate data analyzed using the standard procedure; dashed lines indicate data analyzed using the additional 60 s averaging.

6.3.2 Test material TM-2

A summary of all results obtained for test material TM-2 using the new method is presented in Figure 34. Due to the problems discussed in Section 4.3, emissivity was only obtained for temperature range 200…600 ºC. Within this range, the emissivity of test material TM-2 appears to be independent of temperature.
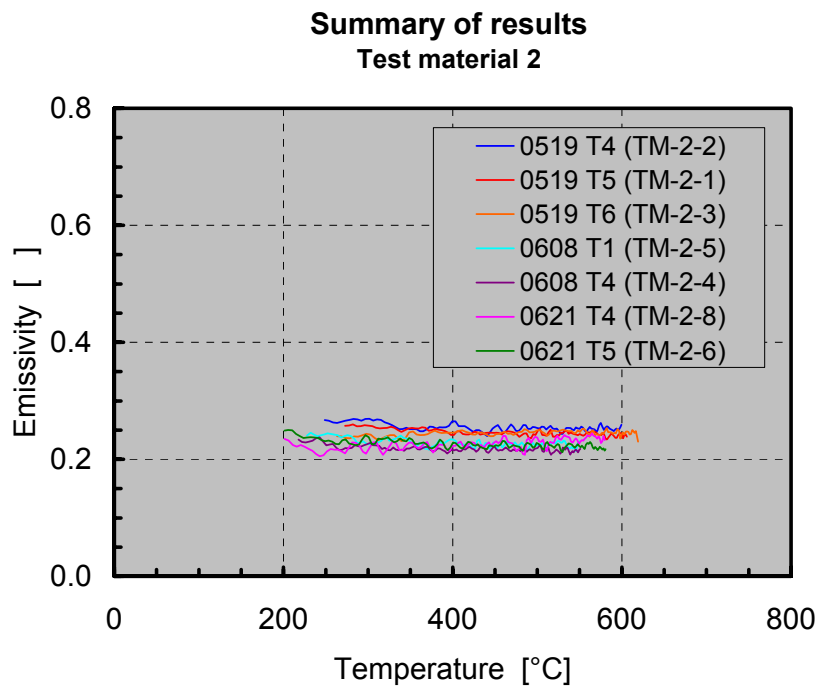
Summary of results
Test material 2

Figure 34. Summary of all results obtained for test material TM-2 using the new method. All data analyzed using the standard procedure.

6.3.3 Test material TM-3

A summary of all results obtained for test material TM-3 using the new method is presented in Figure 35. Due to the problems discussed in Section 4.3, emissivity was only obtained for temperature range 150…550 ºC. At low temperatures, the emissivity of test material TM-3 appears to be fairly low and independent of temperature. At temperatures above 350 ºC the emissivity starts to increase steeply with temperature, until at temperatures above 500 ºC the emissivity seems to become independent of temperature again.

For test material TM-3, the experiments shown in Figure 35 produced good quality data and could be analyzed using the standard procedure. The standard procedure was explained in Section 6.1.6. Two more experiments were carried out with test specimens TM-3-5 and TM-3-6, but the data were noisy and could only be analyzed using the additional 60 s averaging. However, the results obtained this way were not useful and are not shown in Figure 35. The reason is that the emissivity of test material TM-3 appeared to change very rapidly at temperatures above 300 ºC, and the additional 60 s averaging procedure cannot follow such rapid changes, as was discussed in Section 6.1.6.
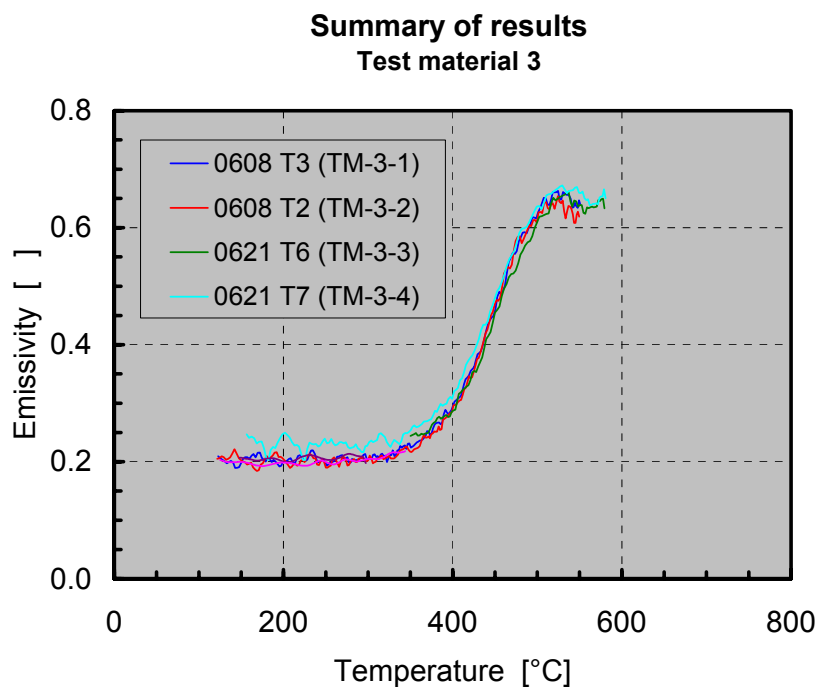

Summary of results
Test material 3

Figure 35. Summary of all results obtained for test material TM-3 using the new method. All data analyzed using the standard procedure.

7. Tests using the existing method

7.1 Equipment and procedure

7.1.1 Equipment for measurements at 100 ºC

The principle of the existing method is shown in Figure 36. The test specimen, which must be metallic and flat, is heated to about 100 °C temperature by pressing it toward a heated aluminum cylinder. The detecting system measures the radiance alternatively from the test specimen and from a blackbody. The latter is also set at 100 °C. The emissivity is calculated in principle by simply taking the ratio of the two detector outputs. However, a few corrections must be made. The procedure for calculating the emissivity from the data is described in Section 7.1.4.

A translational stage is used for the positioning of the test specimen and the blackbody into the optical path of the infrared detector. A tube with a length of about 500 mm is used to ensure that the detector sees both the material to be investigated and the blackbody at the same solid angle. Apertures in the ends of the tube limit the detector field of view; see Figure 37. The tube also shields the detector from radiation from the environment.
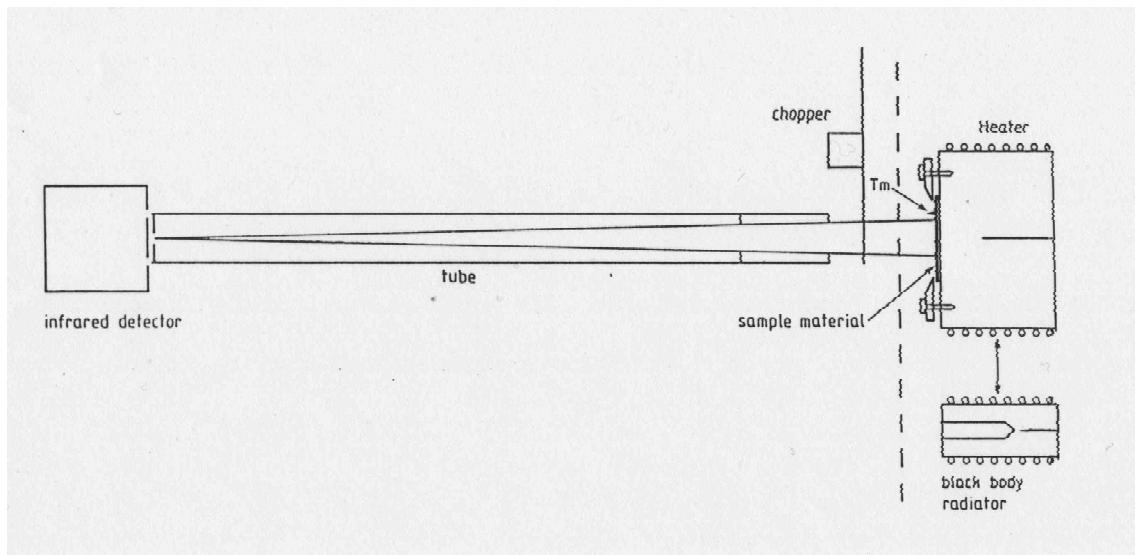

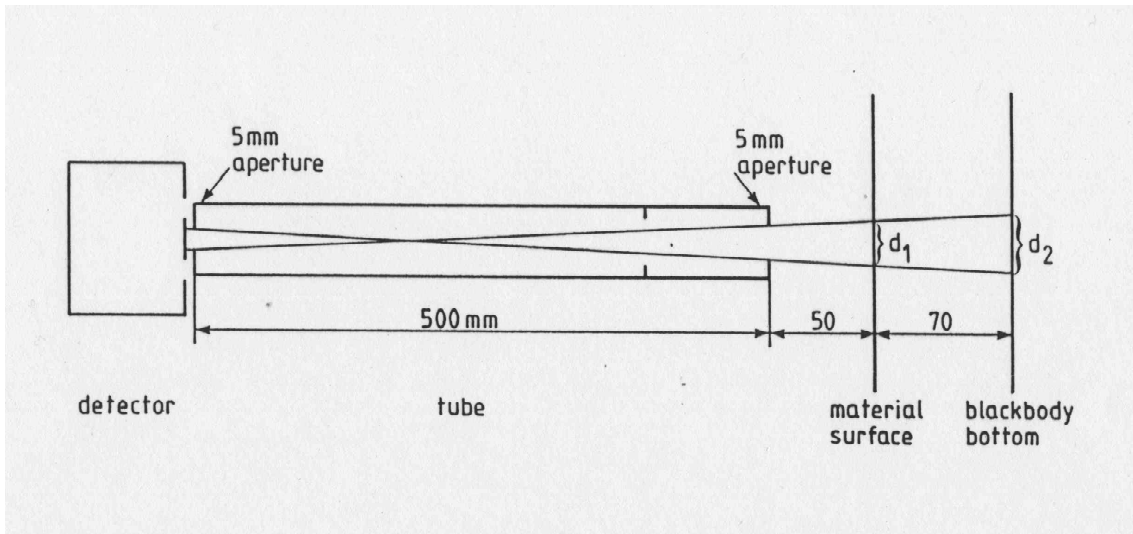*Figure 36. Schematic outline of the existing method (SP method) for the measurement of emissivity at 100 ºC.*

Figure 37. Geometrical dimensions of the detecting set-up.

The blackbody is a cylindrical cavity inside a heated aluminum cylinder as shown in Figure 38. The cavity is 70 mm long and 10 mm in diameter and has a conical bottom. The inside of the blackbody is threaded and painted black giving an emissivity of 0.99 as seen by the detector. A thermocouple, inserted into a well near and behind the cavity, measures the temperature of the blackbody.
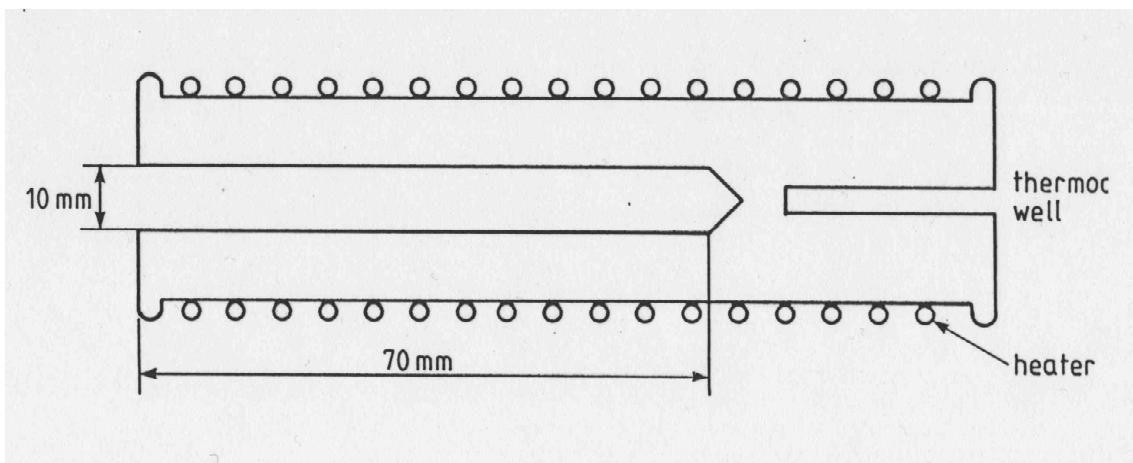

Figure 38. The outline of the blackbody.

The infrared detector, a Golay detector, measures the radiation from a small part, less than 7 mm diameter spot, of the material. The Golay detector requires chopped radiation. It generates an ac-signal which is proportional to the difference of the radiation level with the chopper path open and closed. This signal is amplified by using a lock-in-amplier which is synchronized with the chopper. The Golay detector, which is a pneumatic-thermal-electric device, has a black coated absorber and a KRS5 window giving a relatively flat responsivity in the wavelength range 1 μm–30 μm.

In Figure 39 the Golay detector with its KRS5 window is shown. The absorber in the detector is heated by the radiation and a bulb connected to the absorber expands by the heat. A specular membrane is placed on the other end of the bulb and light from an LED is reflected from the membrane to a photodetector. This detector is reasonably linear and very sensitive. For example, if directed towards a source like a soldering iron, it could be destroyed by excess overloading.

Figure 39. The Golay detector with its reddish KRS5 window. It is inserted into the tube seen to the right.

Figure 40 shows the arrangement for heating the test specimen to 100 °C temperature. The test specimen is pressed towards the end of an aluminum cylinder and the surface temperature, at the spot of the radiance measurement, is measured by usage of a thin thermocouple. To minimize cooling of the thermojunction from the ambient air it is necessary to align the thermocouble thread along the material. At least 20 mm of its end should have contact with the material. The 100 °C blackbody is also shown in the figure.
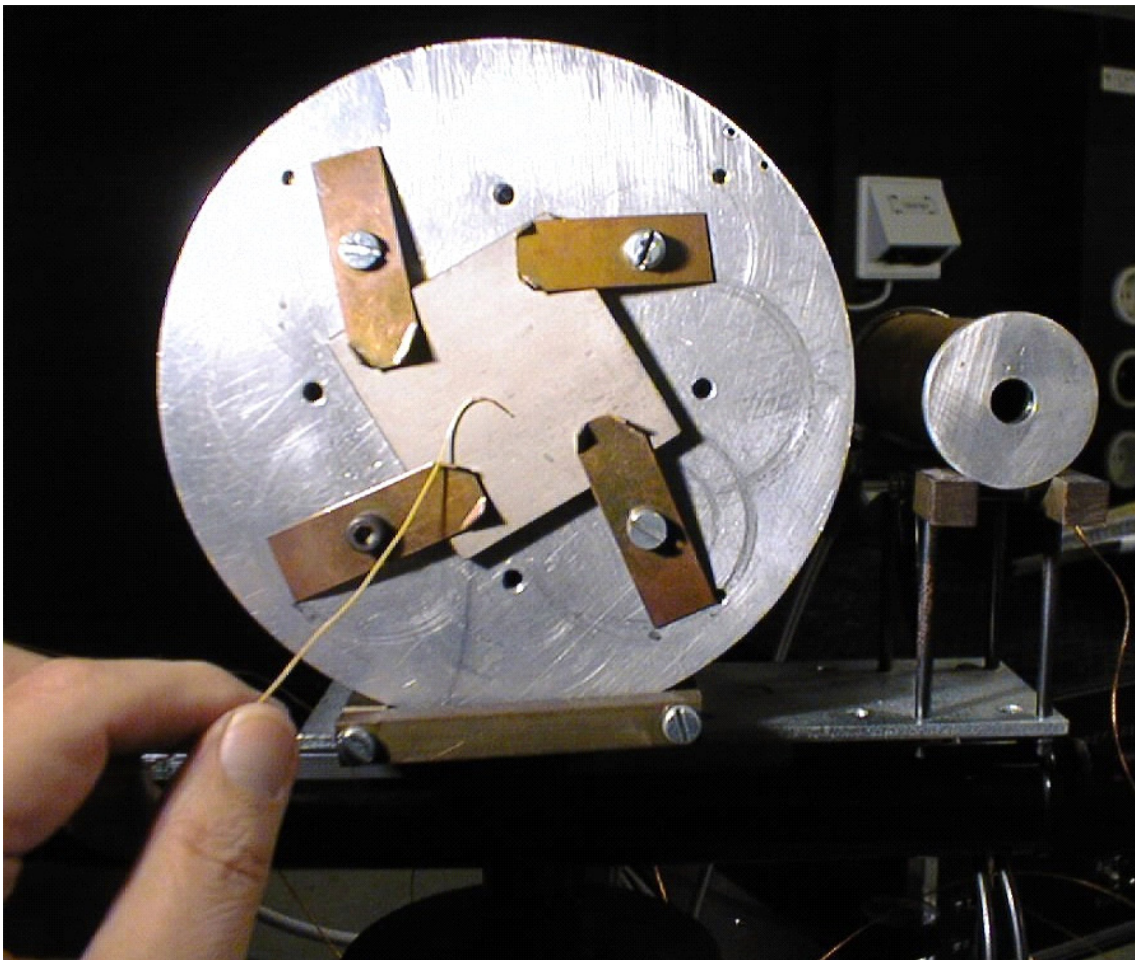

Figure 40. The test specimen attached to the aluminum cylinder used for heating to 100 °C. The surface temperature is measured using a thin thermocouple pressed along the surface. The 100 °C blackbody is shown to the right.

The Golay detector, the tube, and the chopper are fix position on an optical bench, Figure 41 and Figure 42. The sample heater and the blackbody radiator are mounted on a translational stage, i.e. the sample and the output aperture of the blackbody could be alternatively moved into the optical path defined by the tube. If the temperature of the sample is set to be the same as that of the blackbody, the directional normal emissivity of the sample could be calculated simply as the ratio of the two corresponding measured detector outputs.
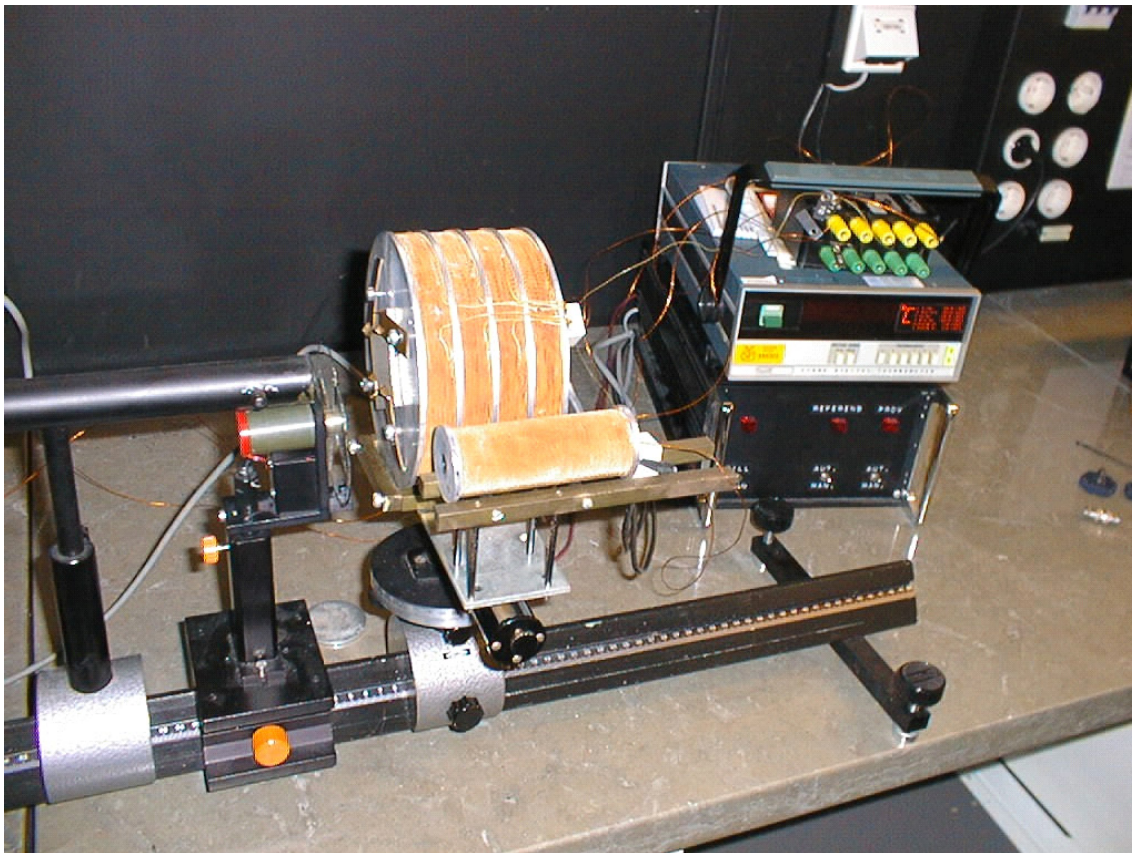
Figure 41. Side view of the sample heater and the blackbody. The right end of the tube and the chopper is to the left. To the right is the heater controller and the thermocouple thermometer together with a thermocouples switch.
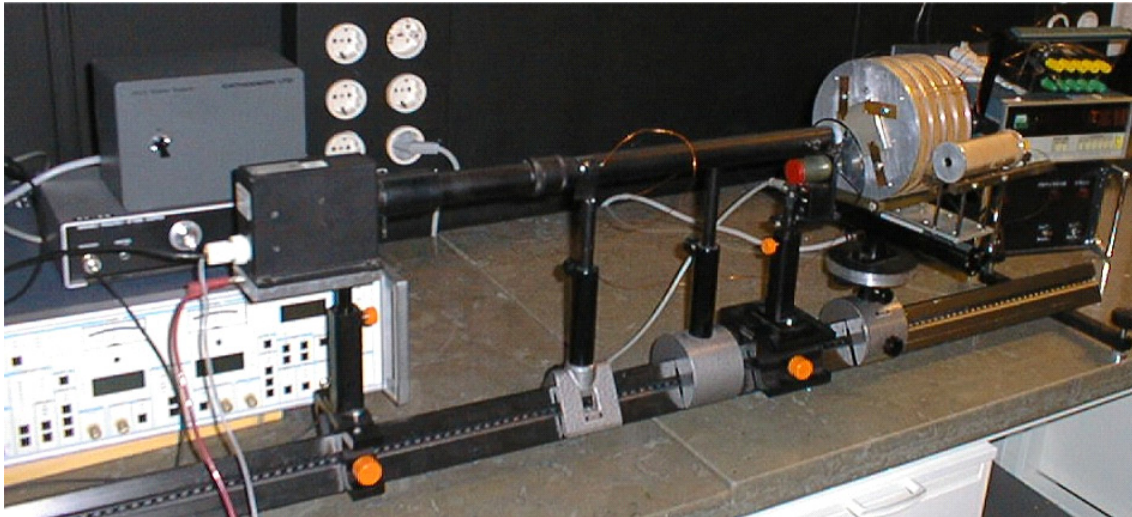
Figure 42. The complete set-up for 100 °C. Behind the detector to the left are from top to bottom the controller of the detector, the controller of the chopper, and the lock-in-amplifier.

A more detailed explanation of the method is described by Sidsten (1979) and by Liedquist (1987). However, the method of measuring the surface temperature, described in these two references, is now modified to be as shown in Figure 40. Instead of drilling holes for the thermocouple leads according to the original method, a thin thermocouple is now used directly. This change was performed by practical reasons and gives better accuracy.

7.1.2 Modification of the method for measurements at 200 °C

As a part of this project, a second aluminum cylinder (Figure 43 and Figure 44) was used which could be set to 200 °C. A 100 mm long and 10 mm wide hole was drilled into the peripheral part of the cylinder. This hole was threaded and painted black inside and served as a 200 °C blackbody. This blackbody was compared to the 100 °C blackbody and found to have an emissivity of 0.99 as well.
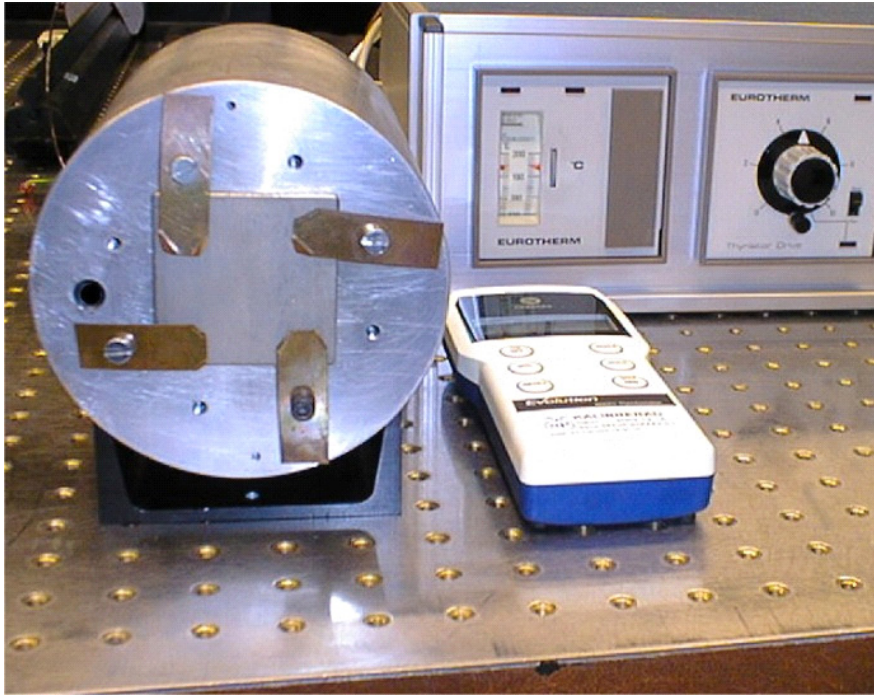
Figure 43. The test specimen attached to the aluminum cylinder used for heating to 200 ℃. The exit output of the 200 ℃ blackbody is seen to the left. To the right is the heater controller and also the thermocouple thermometer used to measure the temperature of the blackbody. The aluminum body is mounted on a computer controlled translational stage (not seen in this figure).
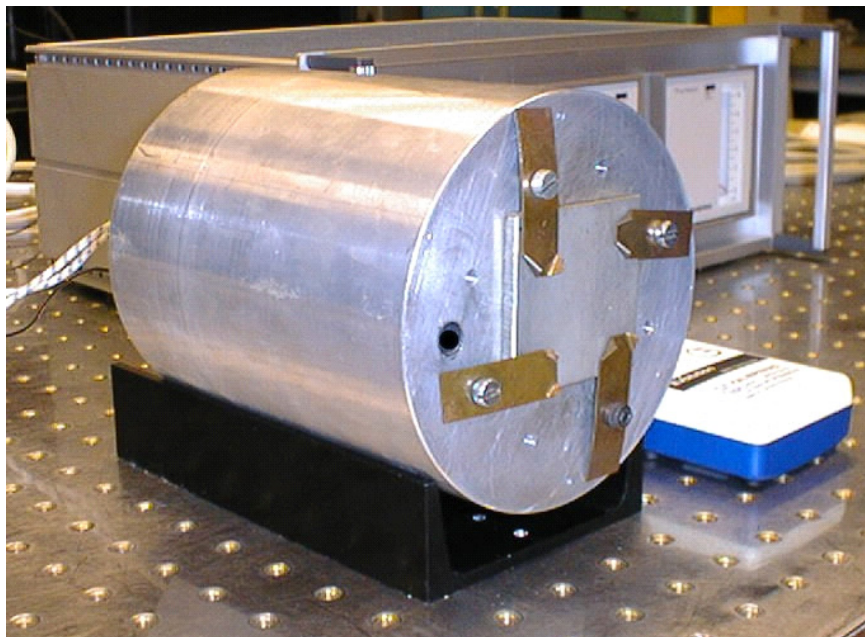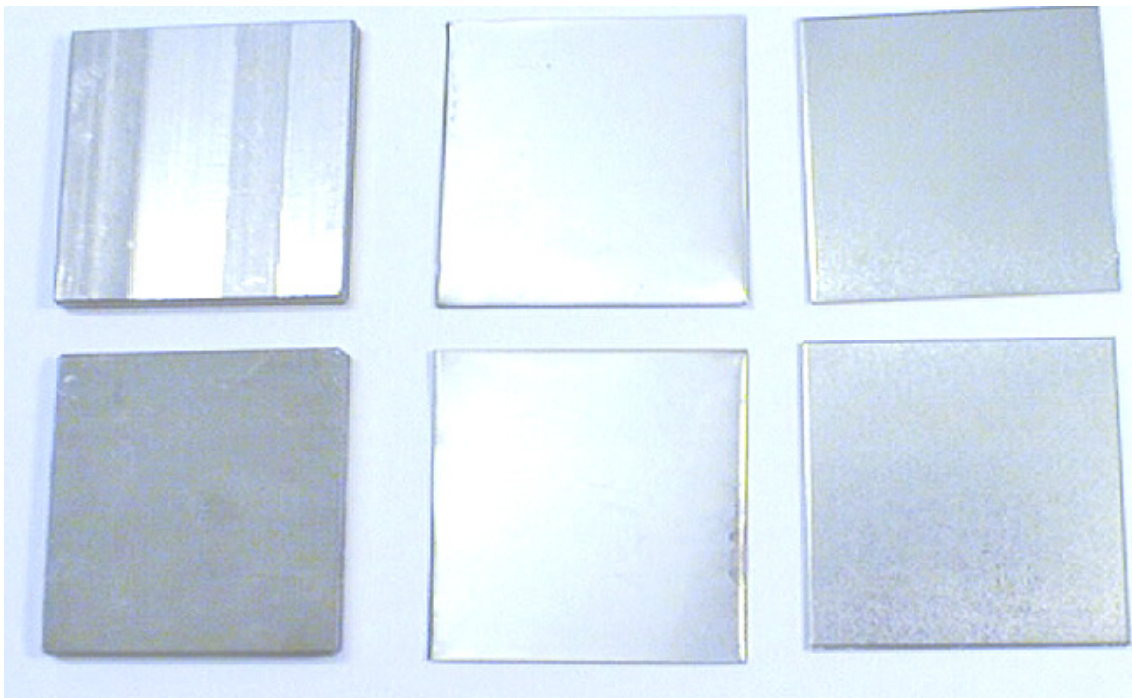

Figure 44. Side view of the 200 ℃ aluminum cylinder.

7.1.3 Test specimens

Seven pieces, about 50 mm x 50 mm, of material TM-1, six pieces TM-2 and three pieces TM-3 were sent from VTT to SP and measured there. Two samples of each material are shown in Figure 10. The lower sample of TM-1 is typical but there could be glossy samples like the top one. TM-2 is more visually glossy than TM-3.

Figure 45. The test materials. From left to right two samples of each TM-1, TM-2, and TM-3.

7.1.4 Data processing

The radiant flux that reaches the detector surface consists basically of four components defined from Stefan-Boltzmann's law which is assumed to be approximately valid. When the material being investigated is placed in the optical path of the infrared detector, the four components are

- the direct outgoing flux from the material with temperature T_m and emissivity ε_m: $\sigma \varepsilon_m T_m^4$

- the flux from the surrounding temperature T_a, reflected by the material towards the detector: $\sigma (1 - \varepsilon_m) T_a^4$

- the flux from the chopper blade having temperature T_c and emissivity ε_c in closed position (subtracted): $\sigma \varepsilon_c T_c^4$

- the internal flux from the tube having temperature T_t, reflected by the chopper blade back to the detector (subtracted): $\sigma (1 - \varepsilon_c) T_t^4$.

The detector signal V_m is proportional to the sum of the first two contributions minus the sum of the two last ones:

$$V_m = c \cdot \left[\varepsilon_m T_m^4 + (1 - \varepsilon_m) T_a^4 - \varepsilon_c T_c^4 - (1 - \varepsilon_c) T_t^4 \right] \tag{35}$$

where c is a proportionality constant.

When the blackbody is placed in the optical path of the detector, the detector signal is

$$V_b = c \cdot \left[\varepsilon_b T_b^4 + (1 - \varepsilon_b) T_a^4 - \varepsilon_c T_c^4 - (1 - \varepsilon_c) T_t^4 \right] \tag{36}$$

where ε_b and T_b are the emissivity and temperature of the blackbody, respectively. As was noted earlier, $\varepsilon_b = 0.99$.

The chopper blade is covered by aluminum foil towards the detector. The foil has very low emissivity. Therefore, ε_c can be set to zero and the final equation is achieved from Equations (35) and (36) by eliminating the proportionality constant c:

$$\varepsilon_m = \varepsilon_b \cdot \frac{V_m}{V_b} \cdot \frac{T_b^4 - T_a^4}{T_m^4 - T_a^4} + (1 - \frac{V_m}{V_b}) \cdot \frac{T_t^4 - T_a^4}{T_m^4 - T_a^4} \tag{37}.$$

7.2 Test results

7.2.1 Normal total emissivity

Using the 100 °C method, all seven test specimens made of material TM-1 and all six test specimens made of material TM-2 were measured five times. Both sides of the test specimens were studied but no significant differences in emissivity between the sides could be found. The standard deviation for the five measurements on each TM-1 varied from 0.003 to 0.009 and for TM-2 from 0.001 to 0.002. The average, standard deviation and width of variation of the mean values of all test specimens are given in Table 3.

Table 3. The average, standard deviation and width of variation of the mean values of all test specimens tested using the 100 ºC method.

Material	Temperature [ºC]	Normal total emissivity [ ]		
		Mean	Standard deviation	Width of variation
TM-1	100	0.441	0.012	0.028
TM-2	100	0.145	0.003	0.008

Using the 200 °C method, two sets of tests were carried out. In the first set of tests, one test specimen made of material TM-1 was measured twice, one test specimen made of material TM-2 was measured three times, and one test specimen made of material TM-3 was measured once. In the second set of tests, each test specimen made of materials TM-1 and TM-2 was measured once and one test specimen made of material TM-3 was measured three times. The average, standard deviation and width of variation of the mean values of all test specimens are given in Table 4.

For the 200 °C method, the variations in the results appeared to be comparable to those observed when the 100 °C method was used, except that one measurement for a test specimen made of material TM-1 gave an exceptionally low emissivity value of 0.183. In this measurement, a glossy part of the test specimen was positioned in the optical

path of the detector. This value was excluded from the computation of the results presented in Table 4. The existence of glossy parts in the surface of test material TM-1 was noted earlier in Chapter 5 and is also illustrated in Figure 8 and in Figure 45.

Table 4. The average, standard deviation and width of variation of the mean values of all test specimens tested using the 200 ℃ method. Standard deviation is not computed for TM-3 due to small number of tests.

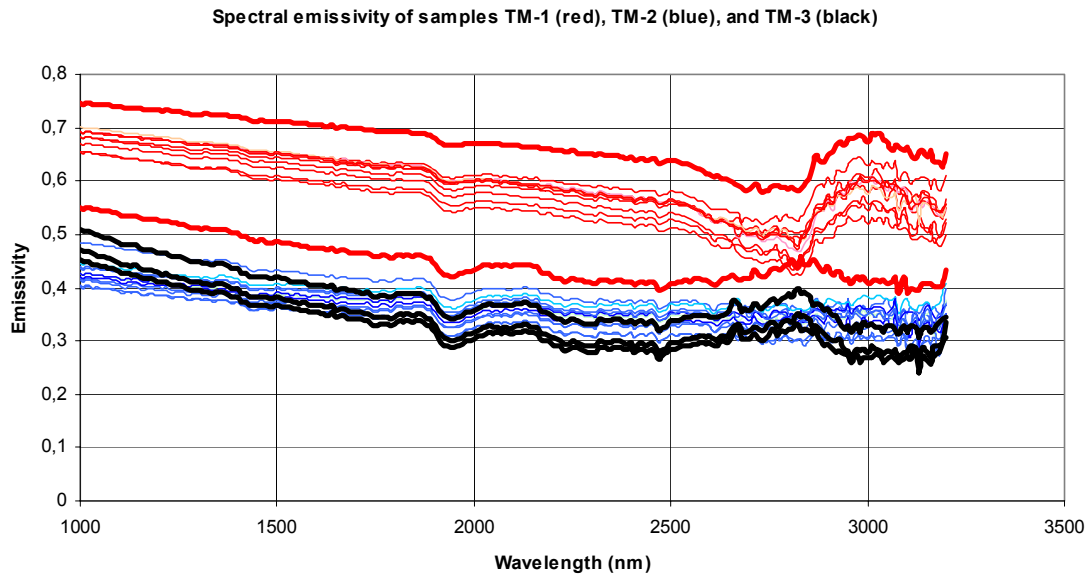| Material	Temperature [ºC]	Normal total emissivity [ ]		
		Mean	Standard deviation	Width of variation
TM-1	200	0.387	0.019	0.049
TM-2	200	0.165	0.005	0.012
TM-3	200	0.070		0.003

7.2.2 Spectral measurements

The spectral reflectance of the test materials was measured with the geometry 8°/t using a PerkinElmer Lambda 900 spectrophotometer in the wavelength range 1000 nm–3200 nm. Only this wavelength range was available at SP at the time being, i.e. only a part of the interesting range 1 μm–30 μm. The test specimens were at a temperature of 25 ºC.

From measured spectral reflectance $\rho(\lambda)$, spectral emissivity was calculated as

$$\varepsilon(\lambda) \quad = \quad 1 - \rho(\lambda) \tag{38}$$

where λ is the wavelength.

The results are shown in Figure 46. Notice the very large spread in the results of test material TM-1.

Spectral emissivity of samples TM-1 (red), TM-2 (blue), and TM-3 (black)

Figure 46. Spectral normal emissivities of the test materials at 25 ºC temperature. Both sides of TM-1 and TM-2 have been measured.

8. Comparison of test results

This chapter presents a summary of the results together with a comparison between the results obtained at VTT using the new method and the results obtained at SP using the existing method.

When the VTT results are compared with the SP results, it must be noted that the VTT method measures the hemispherical total emissivity ε whereas the SP method measures the normal total emissivity ε_N; generally speaking, ε and ε_N are not expected to be equal. The value for the ratio of ε to ε_N can be predicted using the electromagnetic theory as has been described by Siegel and Howell (1972); the results have been compiled in, e.g., Figure 4-8 of Siegel and Howell and Figure 4 on page Ka 5 of VDI-Wärmeatlas (1984). The information presented in these two figures will be used to facilitate the comparison between VTT results and SP results.

8.1 Test material TM-1

The results for test material TM-1 are summarized in Figure 47. For this test material, six successful tests were carried out at VTT (test specimens TM-1-1…TM-1-6), and the results of each individual test are shown. The results obtained at SP are only shown as average values for 100 °C and 200 °C, since the scatter between individual results was extremely small (of the order of 0.01).

The following points should be noted:

- Four of the experiments carried out at VTT produced good quality data and could be analyzed using the standard procedure; these results are shown in Figure 47 using solid lines. Two of the experiments carried out at VTT produced low quality data and had to be analyzed using additional 60 s averaging; these results are shown in Figure 47 using dashed lines. The standard procedure and the additional 60 s averaging were explained in Section 6.1.6. As was discussed in Section 6.1.6, these two methods for data processing are both expected to be appropriate in the case of test material TM-1, whose emissivity appears to be only weakly dependent on temperature.

- In one test at SP, the measured value of emissivity was only 0.183 at 200 °C, apparently due to the fact that an exceptionally glossy part of the test specimen was studied in the test. This low value was excluded from the computation of the average value (cf. Section 7.2.1).

A comparison of results obtained at 200 °C for test material TM-1 shows that the VTT method gave $\varepsilon \approx 0.3...0.35$ and the SP method gave $\varepsilon_N \approx 0.4$. Based on the electromagnetic theory, it should be expected that $\varepsilon / \varepsilon_N \approx 1$ for $\varepsilon_N \approx 0.4$. Thus, the results obtained at VTT are approximately 20 % lower than what should have been expected based on the results obtained using the SP method. It should be kept in mind, however, that the VTT method measures the average emissivity of all surfaces of the test specimen. For test material TM-1, the thickness of the test specimens was 5 mm, and a significant fraction of the total area of each test specimen therefore consisted of new surface which was created when the test specimen was cut from the test material (cf. the discussion in Section 4.5). Furthermore, the newly cut surfaces of test material TM-1 were very glossy and looked quite different from the original surfaces. It seems possible that this factor may have had sufficient influence on the results so as to explain the difference between SP results and VTT results.
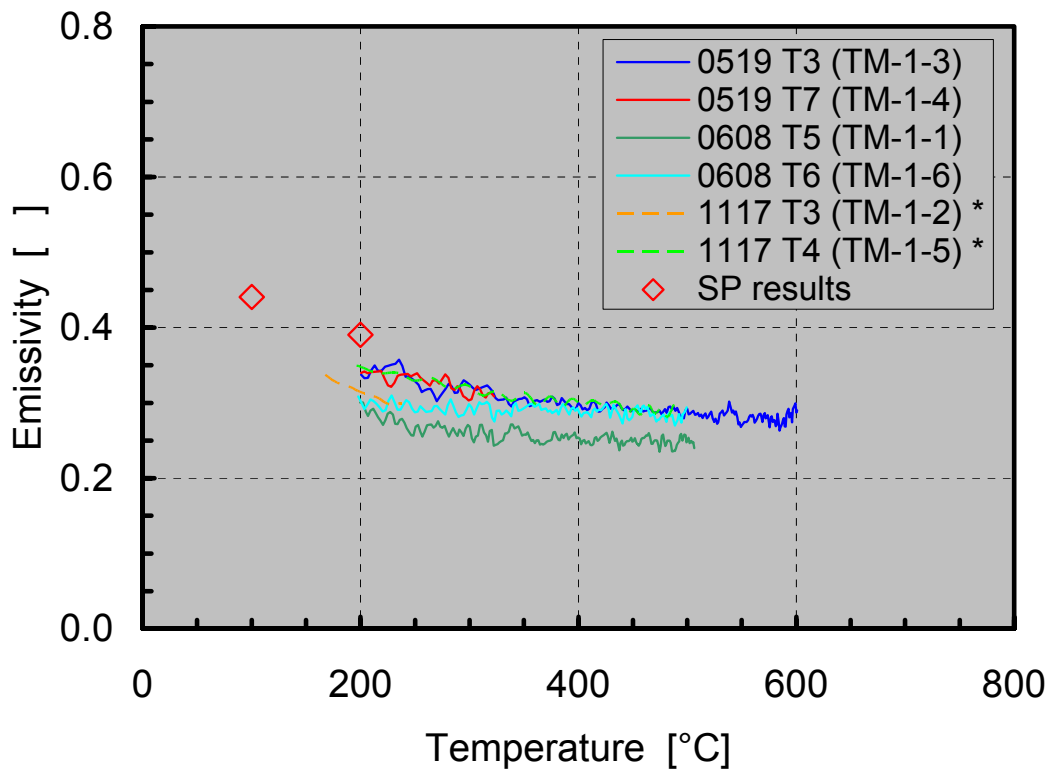

Figure 47. A summary of results obtained for test material TM-1. SP results in the figure are for the normal total emissivity, whereas the other results are for the hemispherical total emissivity.

8.2 Test material TM-2

The results for test material TM-2 are summarized in Figure 48. For this test material, seven successful tests were carried out at VTT (test specimens TM-2-1…TM-2-6, TM-2-8) and the results of each individual test are shown. All experiments produced good quality data and could be analyzed using the standard procedure explained in Section 6.1.6. The results obtained at SP are only shown as average values for 100 ºC and 200 ºC, since the scatter between individual results was extremely small (of the order of 0.01).

A comparison of results obtained at 200 ºC in this study shows that the VTT method gave $\varepsilon \approx 0.22…0.27$ and the SP method gave $\varepsilon_N \approx 0.18$. Based on the electromagnetic theory, it should be expected that $\varepsilon / \varepsilon_N \approx 1.15$ for $\varepsilon_N \approx 0.18$. Thus, the results obtained at SP suggest that the value of ε is approximately $0.18 \cdot 1.15 \approx 0.21$. The uncertainty of the SP result is ±0.03 and the uncertainty of the VTT results is approximately 20 %; thus, the difference in the results appears to be well within the combined uncertainty interval.
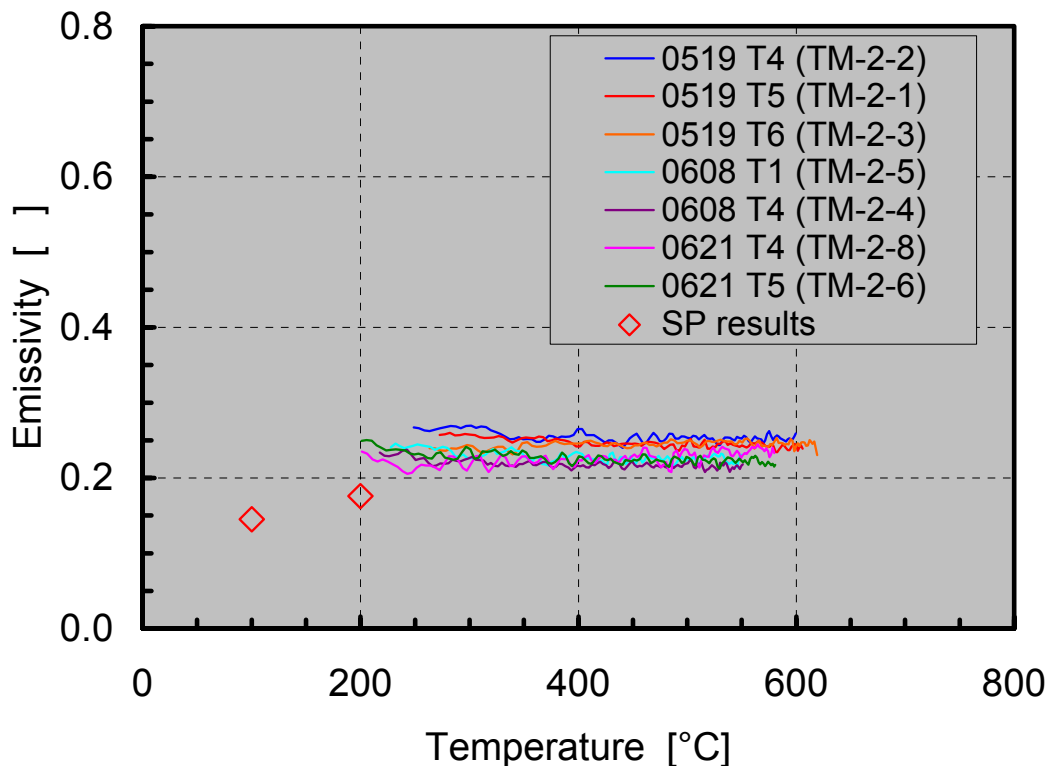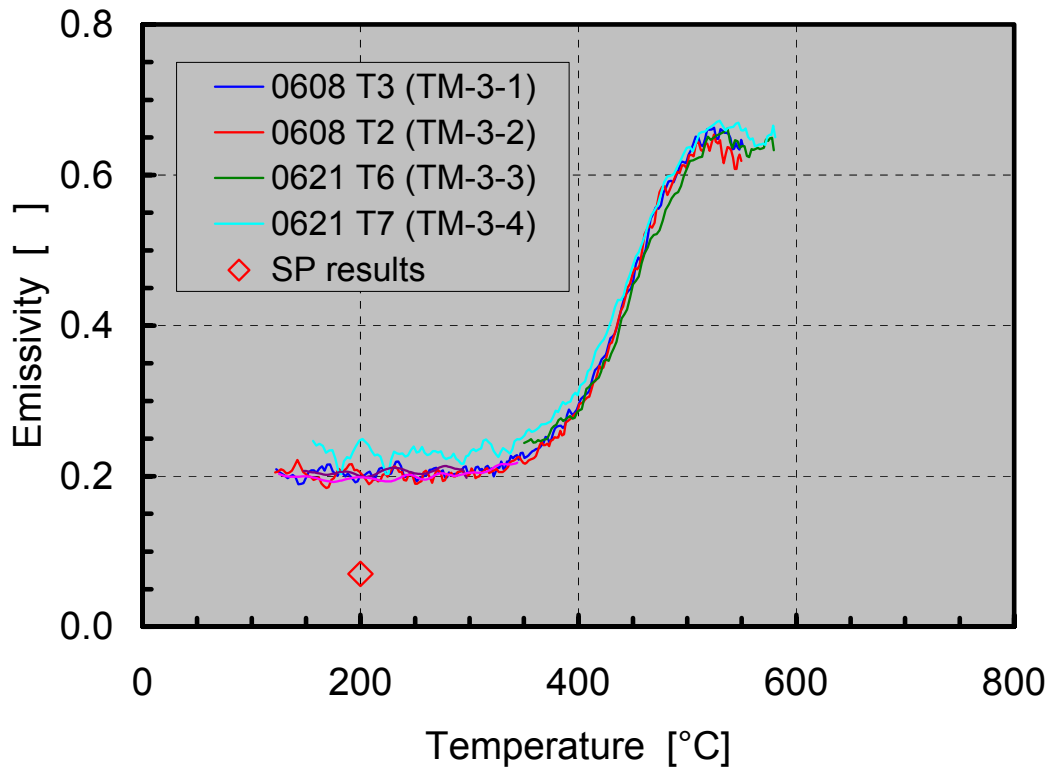

Figure 48. A summary of results obtained for test material TM-2. SP results in the figure are for the normal total emissivity, whereas the other results are for the hemispherical total emissivity.

8.3 Test material TM-3

The results for test material TM-3 are summarized in Figure 49. For this test material, four successful tests were carried out at VTT (test specimens TM-3-1…TM-3-4), and the results of each individual test are shown. The results obtained at SP are only shown as an average value at 200 ºC, since the scatter between individual results was extremely small (of the order of 0.003).

A comparison of results obtained at 200 ºC in this study shows that the VTT method gave $\varepsilon \approx 0.2…0.25$ and the SP method gave $\varepsilon_N \approx 0.07$. Based on the electromagnetic theory, it should be expected that $\varepsilon / \varepsilon_N \approx 1.25$ for $\varepsilon_N \approx 0.07$. Thus, the results obtained at VTT are approximately 2.5 times higher than what should have been expected based on the results obtained using the SP method. The reasons for the difference are not known and should be further investigated. In hindsight it is unfortunate that the existing method was not used for this material at 100 ºC and the number of tests carried out at 200 ºC was smaller than for the other materials.

Figure 49. A summary of results obtained for test material TM-3. SP results in the figure are for the normal total emissivity, whereas the other results are for the hemispherical total emissivity.

9. Summary and conclusions

The objective of this study was to develop a simple and inexpensive method for the determination of the emissivities of various types of steel and other metallic materials as a function of their temperature from room temperature up to temperatures occurring in fires. The method could then be used to produce data for computational analyses of the fire safety of various types of structures.

The method developed in this study is based on the heating of a small test specimen in an electrically heated laboratory furnace. The temperatures of the test specimen and the furnace are measured and recorded using a data logger system. The method is indeed quite simple and inexpensive, but its use is limited to materials which possess a high thermal conductivity and are physically and chemically inert in the temperature range of interest (no melting or other phase transitions, no charring, burning or other chemical reactions). Furthermore, reliable results are only obtained above a minimum temperature, the value of which varies depending on experimental conditions but seems to be in the range from 150 ℃ to 200 ℃.

Three different steel types were used in testing the new method: two stainless steels and one carbon steel. The emissivities of the two stainless steels were determined for the temperature range from approximately 200 ℃ to approximately 600 ℃. The emissivity of the carbon steel was determined for the temperature range from approximately 150 ℃ to approximately 550 ℃.

Uncertainty of the emissivity values obtained with the new method was estimated to be approximately ±20 %. Repeatability of the results was well within the ±20 % limit.

The results were compared with those obtained using a method developed earlier by SP. The SP method gives emissivity at a fixed temperature; earlier the fixed temperature was 100 ℃, but the method was now upgraded so that 200 ℃ also became possible. Thus, emissivity values at 200 ℃ could be used to compare the two methods.

For the two stainless steels, there was good agreement between results obtained using the new method and results obtained using the existing method. For the carbon steel, the differences were much larger than would have been expected. The reasons for the differences have not been found yet and should be further investigated.

References

Chapman, A. J. 1987. Fundamentals of heat transfer. New York: MacMillan Publishing Company. 751 p.

EAL-R2. 1997. Expression of the uncertainty of measurement in calibration. European cooperation for Accreditation of Laboratories. 27 p.

Eurocode 3: Design of steel structures. Part 1.2: General rules. Draft prEN 1993-1-2, February 2002.

Incropera, F. P. & DeWitt, D. P. 2002. Fundamentals of heat and mass transfer. 5th ed. Hoboken: John Wiley & Sons. 981 p.

Laine, J. 1998. Kaasujen ainearvot prosessilaskentaa varten. (Physical properties of gases for process computations.) Helsinki: Otatieto. 50 p. (In Finnish.)

Lewis, J. R. 1977. Physical properties of stainless steels. In: Peckner, D. & Bernstein, I. M. (eds). Handbook of stainless steels. New York: McGraw-Hill. Pp. 19–1...19–36.

Liedquist, L. 1987. A radiometric method for measurement of emissivity of metallic surfaces. Non Nuclear Energies Workshop on Optical Property Measurement Techniques, Ispra, 27–29 Oct 1987, pp. 277–280.

Sidsten, M. 1979. A radiometric method for the measurement of emissivity. Thesis LITH-IFM-EX-128, Linköping University. 32 p. (In Swedish.)

Siegel, R. & Howell, J. R. 1972. Thermal radiation heat transfer. New York: McGraw-Hill. 814 p.

VDI-Wärmeatlas, 4. Auflage. 1984. VDI-Verlag, Düsseldorf. ISBN 3-18-400415-5.

Author(s)	
Paloposki, Tuomas & Liedquist, Leif	

Title

Steel emissivity at high temperatures

Abstract

A new test method was developed at VTT for the determination of the emissivities of different types of steel and other metallic materials as a function of the temperature of the material. The method is simple and inexpensive, but its use is limited to materials which possess a high thermal conductivity and are physically and chemically inert in the temperature range of interest (no melting or other phase transitions, no charring, burning or other chemical reactions). Furthermore, reliable results are only obtained above a minimum temperature, the value of which varies depending on experimental conditions but seems to be in the range from 150 ºC to 200 ºC.

Three different steel types were used in testing the new method: two stainless steels and one carbon steel. The emissivities of the two stainless steels were determined for the temperature range from approximately 200 ºC to approximately 600 ºC. The emissivity of the carbon steel was determined for the temperature range from approximately 150 ºC to approximately 550 ºC.

Uncertainty of the emissivity values obtained with the new method was estimated to be approximately ±20 %. Repeatability of the results was well within the ±20 % limit.

The results were compared with those obtained using a method developed earlier by SP. The SP method gives emissivity at a fixed temperature; earlier the fixed temperature was 100 ºC, but the method was now upgraded so that 200 ºC also became possible. Thus, emissivity values at 200 ºC could be used to compare the two methods.

For the two stainless steels, there was good agreement between results obtained using the new method and results obtained using the existing method. For the carbon steel, the differences were much larger than would have been expected. The reasons for the differences have not been found yet and should be further investigated.

Författarna
Paloposki, Tuomas & Liedquist, Leif

Namn

Stålets emissivitet vid höga temperaturer

Referat

En ny provmetod har utvecklats hos VTT för mätning av emissivitet hos olika sorter av stål och andra metaller. Emissiviteten mäts som funktion av materialets temperatur. Metoden är enkel och billig, men kan endast tillämpas för materialer som har hög värmekonduktivitet och som är fysikaliskt och kemiskt passiva, dvs som inte genomgår smältning eller andra fastransformationer och som inte förkolnas, bränns eller deltar i andra kemiska reaktioner. Härtill kan pålitliga resultat endast nås ovanför en minimumtemperatur, som varierar enligt provförhållanden men verkar vara ungefär 150…200 ºC.

Tre olika sorter av stål användes i testerna: två typer av rostfritt stål och ett byggnadsstål. För de två typerna av rostfritt stål, mättes emissiviteter inom temperaturområdet 200…600 ºC och för byggnadsstålet inom temperaturområdet 150…550 ºC.

Osäkerheten i emissivitetsvärden som mättes med den nya metoden uppskattades vara ungefär ±20 %. Reproducerbarheten var tydligt inom de här gränserna.

Resultaten jämfördes med de resultat som nåtts med en existerande metod tidigare utvecklad hos SP. Den existerande metoden producerar emissivitetsvärden vid en bestämd temperatur; tidigare var den bestämda temperaturen 100 ºC, men nu utvecklades metoden så att emissiviteten kan också mätas vid 200 ºC. Så blev det möjligt att jämföra resultat som nåtts med de två metoderna.

För de två typerna av rostfritt stål, passade resultaten som nåtts med den nya metoden bra ihop med resultaten som nåtts med den existerande metoden. För byggnadsstålet var skillnaderna större än väntat. Orsakerna till skillnaderna är inte ännu kända och borde studeras.

A new test method was developed at VTT for the determination of the emissivities of different types of steel and other metallic materials as a function of the temperature of the material. The method is simple and inexpensive, but has a few limitations. The results obtained with the new method were compared with those obtained using a method developed earlier by SP. For two stainless steels, there was good agreement between results obtained using the new method and results obtained using the existing method. For a carbon steel, the differences were much larger than would have been expected.